Atmospheric Research 200 (2018) 36–59

Contents lists available at ScienceDirect

Atmospheric Research

journal homepage: www.elsevier.com/locate/atmosres

Impact of SST on heavy rainfall events on eastern Adriatic during SOP1 of HyMeX

Stjepan Ivatek-Šahdan[a], Antonio Stanešić[a], Martina Tudor[a,*], Iris Odak Plenković[a], Ivica Janeković[b,c]

[a] Croatian Meteorological and Hydrological Service, Grič3, Zagreb, Croatia
[b] Rudjer Bošković Institute, Bijenička 54, Zagreb, Croatia
[c] The University of Western Australia, School of Civil, Environmental and Mining Engineering & UWA Oceans Institute, Crawley, WA 6009, Australia

A R T I C L E I N F O

Keywords:
Intensive precipitation events
Sea surface temperature
Numerical weather prediction

A B S T R A C T

The season of late summer and autumn is favourable for intensive precipitation events (IPE) in the central Mediterranean. During that period the sea surface is warm and contributes to warming and moistening of the lowest portion of the atmosphere, particularly the planetary boundary layer (PBL). Adriatic sea is surrounded by mountains and the area often receives substantial amounts of precipitation in short time (24 h). The IPEs are a consequence of convection triggered by topography acting on the southerly flow that has brought the unstable air to the coastline. Improvement in prediction of high impact weather events is one of the goals of The Hydrological cycle in the Mediterranean eXperiment (HyMeX). This study examines how precipitation patterns change in response to different SST forcing. We focus on the IPEs that occurred on the eastern Adriatic coast during the first HyMeX Special observing period (SOP1, 6 September to 5 November 2012). The operational forecast model ALADIN uses the same SST as the global meteorological model (ARPEGE from Meteo France), as well as the forecast lateral boundary conditions (LBCs). First we assess the SST used by the operational atmospheric model ALADIN and compare it to the in situ measurements, ROMS ocean model, OSTIA and MUR analyses. Results of this assessment show that SST in the eastern Adriatic was overestimated by up to 10 K during HyMeX SOP1 period. Then we examine the sensitivity of 8 km and 2 km resolution forecasts of IPEs to the changes in the SST during whole SOP1 with special attention to the intensive precipitation event in Rijeka. Forecast runs in both resolutions are performed for the whole SOP1 using different SST fields prescribed at initial time and kept constant during the model forecast. Categorical verification of 24 h accumulated precipitation did not show substantial improvement in verification scores when more realistic SST was used. Furthermore, the results show that the impact of introducing improved SST in the analysis on the precipitation forecast varies for different cases. There is generally a larger sensitivity to the SST in high resolution than in the lower one, although the forecast period of the latter is longer.

1. Introduction

Intensive precipitation events (IPEs) of more than 100 mm in 24 h are regularly recorded over the region of central Mediterranean. These events can lead to flash floods and cause substantial damages and occasionally human casualties (Silvestro et al., 2012; Rebora et al., 2013; Ivančan-Picek et al., 2014). The most severe IPEs are often associated to synoptic situations with blocking when weather systems are more stationary in space and time (Doswell et al., 1996; Homar et al., 2002). The mountains surrounding the Adriatic can trigger or enhance stationary mesoscale convective system (MCS) associated to southerly flow advecting moist air from the Mediterranean/Adriatic Sea (Ivančan-Picek et al., 2014; Mastrangelo et al., 2011). The conditional convective instability is increased by the moisture and heat released by the warm sea in late summer and autumn.

Small et al. (2008) give an overview of the air-sea interaction over fronts and eddies and find that surface stress is positively correlated with SST. The atmospheric boundary layer over ocean responds to the surface heat fluxes by forming an internal boundary layer, differences in turbulent transfer of momentum, hydrostatic pressure anomalies and change in boundary layer height.

Mesoscale SST data improve the representation of heat fluxes at the interface of atmosphere and sea (Weill et al., 2003). Several studies have examined the role of SST in the rainfall events over the central

* Corresponding author.
E-mail address: tudor@cirus.dhz.hr (M. Tudor).

http://dx.doi.org/10.1016/j.atmosres.2017.09.019
Received 19 April 2017; Received in revised form 25 August 2017; Accepted 22 September 2017
Available online 02 October 2017

Mediterranean (Davolio et al., 2016; Stocchi and Davolio, 2016) and more have focused on the western Mediterranean (Romero and Ramis, 1997; Pastor et al., 2001; Lebeaupin et al., 2006) using numerical weather prediction models. Generally, evaporation and convection are more intensive with higher SST, but shifting SST by a fixed amount can also yield a shift in the position of the maximum rainfall (Stocchi and Davolio, 2016). In a recent study of the role of the SST in IPEs in the Ligurian Sea, Cassola et al. (2016) analyze numerical simulations of MCSs using coarse and high resolution SST data and find that the effect of the SST on the location of the peak precipitation intensity is rather limited due to the prevailing influence of topography.

The fluxes of heat and moisture at the air-sea interface contribute to warming and moistening of the PBL. That destabilizes the air mass and can trigger convection. The statistical relationship of the maximum intensity of the tropical cyclones on SST exists in data but it is not reproduced by the climate models (Strazzo et al., 2016) due to low resolution or too strong wind shear in the models. Cold SST can suppress convection over the sea, but it does not vanish completely from the model forecast. These effects vary from case to case and can have negligible impact in the first 12 h (Romero and Ramis, 1997). Sensitivity tests have been performed using hydrostatic models with parametrized convection and high resolution non-hydrostatic models (Pastor et al., 2001; Lebeaupin et al., 2006) where convection is considered explicitly resolved. The precipitation forecast can be significantly improved when SST field is based on measurements (Pastor et al., 2001). Also, a direct relation of the simulated precipitation to the areal averaged SST has been suggested (Pastor et al., 2001).

From 6 September to 5 November 2012, the first Special Observing Period (SOP1) of the HYdrological cycle in the Mediterranean eXperiment (HyMeX) programme was performed (Drobinski et al., 2014) with an aim to improve understanding and forecast of intensive rainfall in the Mediterranean region (Ducrocq et al., 2014). Since one of the goals of HyMeX is to improve the ability of numerical weather prediction (NWP) models in forecasting the location and intensity of heavy precipitation events in the Mediterranean, we focus on the SOP1 to investigate the influence of SST on the forecast of IPE.

Heavy precipitation events often affect the eastern Adriatic coastline leading to flash floods and extensive damages (Mazzocco Drvar et al., 2012; Ivančan-Picek et al., 2014). The local mountains, Dinaric Alps, are arranged parallel to the coastline with peaks more than 1.5 km high, less than 10 km from the shore (Fig. 1). The Alps on the north have a profound influence on the atmospheric motions in the area by orographic cyclogenesis while local mountains (Dinaric Alps) provide orographic uplift and trigger heavy precipitation. The Mediterranean and particularly the Adriatic Sea are sources of moisture and heat for the air mass that is subsequently transported towards the mountains.

High SSTs are usually associated with increased convection and more intensive precipitation (Trenberth and Shea, 2005) in high latitudes and in the tropics where intensive precipitation can be a consequence of sharp SST gradients (Toy and Johnson, 2014). However, Trenberth and Shea (2005) also show negative correlation between SST and precipitation for mid-latitudes and Mediterranean in summer.

Most of operational NWP models keep the initial values of SST throughout the model forecast. This is not realistic in situations when the air-sea fluxes are intensive over small, enclosed and shallow basins, such as the Adriatic sea (Davolio et al., 2015). The SST initialization represents a critical issue for an accurate description of surface fluxes at least for the severe events of intensive precipitation. An accurate description of surface fluxes (above sea surface) depends on the SST used in initial conditions (Davolio et al., 2015) as it does not change during the model forecast (Stocchi and Davolio, 2016). Evolution of SST during the model forecast was found to have weak influence on the atmospheric fields, other than the sensible and latent heat fluxes (Ricchi et al., 2016; Davolio et al., 2017) for the period of severe winter conditions with strong bura wind.

The low level flow over the sea surface is influenced by the SST that modifies its thermodynamic profile. When this flow approaches a mountain that is preceded by a valley the position of precipitation maximum depends on several factors. As distinguished by Davolio et al. (2016), depending on the thermodynamic profile of the atmospheric flow, convection can be triggered upstream of the mountain when the flow is forced to rise over a preexisting cold air pool (over the valley) before the mountain and the heavy rain is localized over the plain. On the other hand, if this convection does not develop over the valley (due to absence of the cold air pool or thermodynamic profile of the impinging air that supports flow over conditions), then heavy rain affects the mountains.

The location of the most extreme rain events can change due to changed SST (Berthou et al., 2014, 2015) on longer timescales (longer than one day but shorter than one month) that de facto changed dynamical environment (wind speed and pressure). The air sea fluxes of heat and momentum over the Adriatic Sea are strongest in bura events in the areas of the strongest jets (Dorman et al., 2007) when the feedback of the atmosphere and the ocean is important, as shown in numerical simulations (Pullen et al., 2003, 2006, 2007). The SST forecast improved in the coupled model run (Pullen et al., 2006) for an intensive cooling event due to the strong wind that stabilized the atmosphere, reduced mixing in the atmosphere and produced more realistic 10 m wind at Italian stations (downwind from the Adriatic Sea during bura).

Intense bura events over the Adriatic lead to intense precipitation events over the Apennines (Ricchi et al., 2016; Davolio et al., 2017). A statistical relationship was found for high precipitation events (HPEs) and SST for several areas over the western Mediterranean (Berthou et al., 2016), but these areas have longer fetch over the sea surface upstream than is achieved over the Adriatic. Few days after an intense air-sea exchange event, a HPE occurred over the western Mediterranean during HyMeX SOP1, while there were also several HPEs that were not preceded by intense air sea fluxes (Rainaud et al., 2016). The discrepancies in the near surface meteorological parameters between the model and measurements are attributed to the usage of fixed SST and overestimation of the sensible heat flux by the model.

Interpolation methods that use less input points applied to SST perform better close to coastlines (Senatore et al., 2014). The SST variations by 0.5 °C are important only in weather conditions when the movement of the weather front is modified sufficiently to affect the enhancement of precipitation by the coastal mountains.

Sudden and intensive cold air outbreaks and cold and dry wind such as bura (Grisogono and Belušić, 2009) can reduce SST by several degrees on a time scale of less than one day. Allowing SST to change during the forecast run could improve the forecast, and forecast quality is rather important in such severe weather events. We do not perform such a test in this paper, but identify cases and areas where it could be important. Previous studies were mostly focused on precipitation over the western Mediterranean, while Adriatic studies focused on bura cases and periods.

The purpose of this study is to evaluate SST used in the operational forecast first. Based on this evaluation, a set of tests is performed with forecast runs where we artificially modify SST field. We further examine the sensitivity of 8 km and 2 km resolution forecasts of IPEs on eastern Adriatic coast that occurred during HyMeX SOP1 to the SST from global analysis and ROMS ocean model.

All experiments are performed using ALADIN (Aire Limitée Adaptation Dynamique développement InterNational, ALADIN International Team, 1997) limited area model (LAM). The reference simulations for the whole period are operational forecasts (Tudor et al., 2013) that use SST from the initial file of the global model ARPEGE (Action de Recherche Petite Echelle Grande Echelle), that was operational at the time (Météo France, 2012). The operational forecasts do simulate IPEs (Ivančan-Picek et al., 2016), but the 8 km resolution forecast puts the peak intensity of precipitation over mountains inland from Rijeka. On the other hand, the operational high resolution run does forecast IPE for Rijeka, but tends to overestimate precipitation in

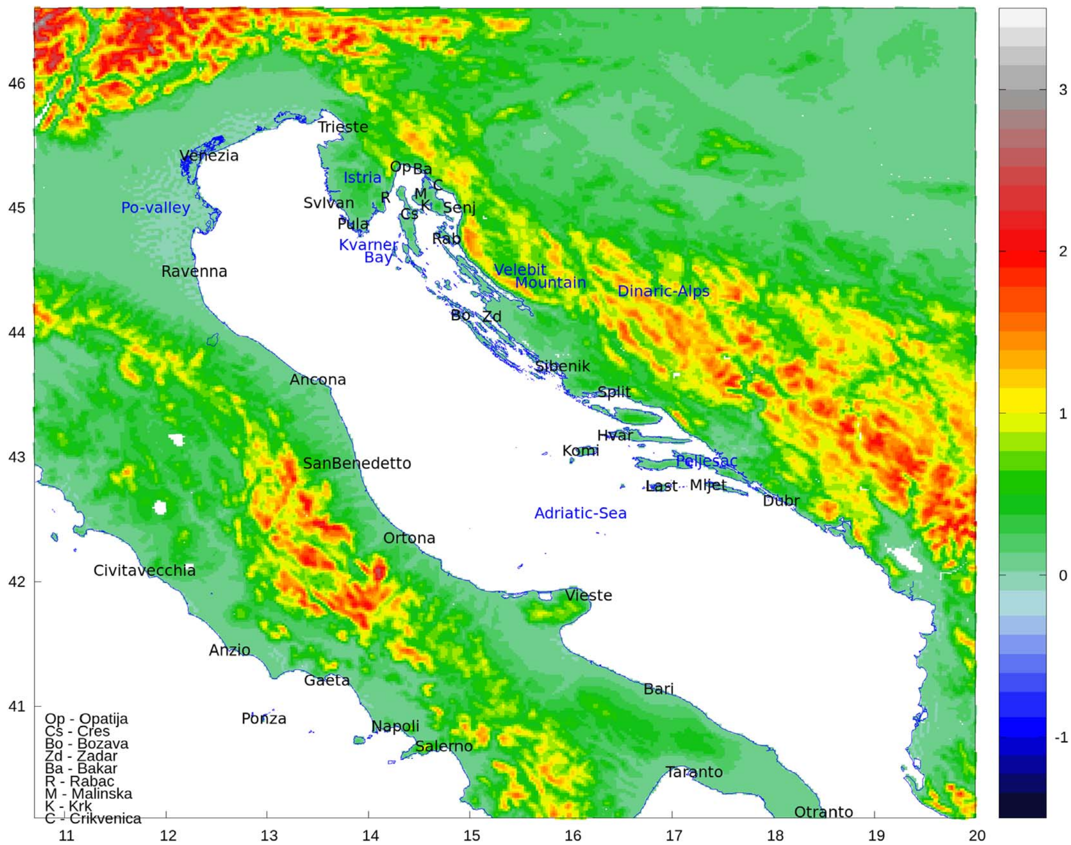

Fig. 1. Map of Adriatic and Italian area with the locations of in situ SST measurements (in black). The names of stations in Croatia are truncated due to large spatial density and explained in the lower left corner in the figure. The background is terrain height (in km) from 2 km resolution ALADIN file, white means that land-sea mask is zero (sea or lake point in the model). The city of Rijeka is between Op and Ba stations and Velebit channel is the narrow channel southeast of the Velebit mountain.

certain areas, such as the Velebit mountain, particularly its southern part. First, several experiments are performed where the SST in the analysis is shifted by a fixed value. Then another set of experiments is performed in which the SST in the analysis is replaced by SST from The Operational Sea Surface Temperature and Sea Ice Analysis (OSTIA, UK Met Office, 2005) and the Multiscale Ultrahigh Resolution (MUR, JPL MUR MEaSUREs Project, 2015) analyses and then from the ROMS (Janeković et al., 2014) ocean model. The sensitivity of simulated precipitation to SST is then evaluated by comparing the results from experiments that use different SST fields to the reference operational forecast.

Here we perform the following tasks for the Adriatic area

- evaluate SST fields from the global atmospheric model, analysis and regional ocean model,
- evaluate model precipitation changes due to uniform shift in SST based on the previous analysis,
- and model precipitation changes due to more realistic SST based on analyses and ocean model forecast.

The above mentioned analysis is focused on the whole SOP1 period (not on bura cases that dominate the analyses published so far).

The statistical parameters are computed in order to see if different SST in the initial conditions can bring improvements in the precipitation forecast (as seen from the statistics point of view).

The paper is organized as follows. The model simulations and characteristics of different SST fields used in experiments are described in Section 2. Section 3 describes the results of simulations using different SST fields. The discussion and summary are in Section 4.

2. Methodology and data

The main objective of this study is to examine how precipitation patterns change in response to different SST forcing for IPEs. Our model simulations cover the entire HyMeX SOP1 period: from 6 September to 5 November 2012 when 8 events with precipitation exceeding 100 mm in 24 h over eastern Adriatic occurred (Ivančan-Picek et al., 2016). Operationally, at the time of HyMeX SOP1, SST was taken from the operational forecast of the global model ARPEGE, that was also used for the forecast lateral boundary conditions. The effect of SST on precipitation forecast was first analyzed by increasing or decreasing the SST by a fixed amount. The subsequent set of experiments used SST from OSTIA and MUR analyses and ROMS ocean model. We focused on IPEs that occurred during HyMeX SOP1, which took place in late summer and autumn 2012, and provided a number of IPEs on eastern Adriatic associated with orographic triggering of convection and extensive stratiform rainfall.

2.1. SST data

In this study we used SST measured insitu at a number of stations in Croatia and Italy (Fig. 1), OSTIA and MUR analyses as well as ROMS model output. Data measured insitu are used to evaluate how well SST from different sources represents SST on eastern Adriatic, which contains numerous islands.

2.1.1. Operational SST

The initial SST fields used for the ALADIN operational forecast in 8 km and 2 km resolutions are taken from the initial file of the ARPEGE operational forecast. ARPEGE (Météo France, 2012) computes weather forecast on a stretched grid. Therefore, the horizontal resolution is variable over the globe, with the highest resolution over France. The LBC files are distributed on a Lambert conformal grid in horizontal resolution of 10.6 km. The ARPEGE operational SST analysis combines Advanced Very High Resolution Radiometer (AVHRR) satellite data and insitu measurements in the operational oceanographic model Mercator (Bahurel et al., 2004). However, in a case of operational failure there were some alternatives used. In situ SST reports by ships and buoys are combined with NCEP SST analysis or a previous analysis (from 6 h before) (Météo France, 2012). If everything else fails, Reynolds global climatology (1° resolution) or European Centre for Medium Range Weather Forecast (ECMWF) SST analysis (Lebeaupin et al., 2006) can be used.

2.1.2. Analyzed SST in 0.05°(6.5 km) resolution - OSTIA

The OSTIA analysis (UK Met Office, 2005; Donlon et al., 2012; Stark et al., 2007) is produced daily on an operational basis at the UK Met Office using optimal interpolation (OI) on a global 0.054° grid. As input, it uses satellite data from the AVHRR, the Advanced Along Track Scanning Radiometer (AATSR), the Spinning Enhanced Visible and Infrared Imager (SEVIRI), the Advanced Microwave Scanning Radiometer-EOS (AMSRE), the Tropical Rainfall Measuring Mission Microwave Imager (TMI), and insitu data from buoys. It is designed as support for the SST data assimilation into NWP models.

2.1.3. Analyzed SST in 0.01°(1 km) resolution - MUR

The MUR SST analysis is produced as near-real-time data set (one day latency) at the Jet Propulsion Laboratory (JPL) Physical Oceanography Distributed Active Archive Center (DAAC) using wavelets as basis functions in an optimal interpolation approach on a global 0.01° grid (Chin et al., 1998; JPL MUR MEaSUREs Project, 2015). As input, it uses skin and sub skin SST observations from the NASA Advanced Microwave Scanning Radiometer-EOS (AMSRE), the Moderate Resolution Imaging Spectroradiometer (MODIS) on the NASA Aqua and Terra platforms, the US Navy microwave WindSat radiometer, AVHRR and insitu SST observations from the NOAA.

2.1.4. ROMS model SST

Aside from SST analyses described before, SST from the Regional Ocean Modelling System (ROMS, Shchepetkin and McWilliams, 2005, 2009) is used over the Adriatic Sea with OSTIA analysis over the rest of the Mediterranean. The ROMS is run for the Adriatic region (Janeković et al., 2014) using Adriatic forecasting System (AFS) AREG lateral boundary conditions at the Otranto Strait that is in turn nested inside the Mediterranean Forecasting System (MFS, Oddo et al., 2006). The model grid has 2 km spatial resolution and 20 s-levels in the vertical. The vertical resolution is increased in the surface layers and bathymetry is computed using Dutour Sikirić et al. (2009). Fresh water sources are computed using more realistic values (Janeković et al., 2014) than former climatology (Raicich, 1994), which overestimates river fluxes.

2.1.5. SST measured in situ

In this study we use SST measured insitu on a number of stations in Croatia and Italy. The SST is measured on a number of stations on the Adriatic, including a number of stations on the islands (Fig. 1). Most of the stations on eastern Adriatic coast are the regular "climate" stations, which measure SST in conventional way at 7, 14 and 21 h local time (at 06, 13 and 20 UTC) each day. These stations are Božava, Sv Ivan na pučini, Komiža, Krk, Lastovo, Mljet, Opatija, Pula, Rab, Rabac, Senj, Šibenik, Split, Zadar, Dubrovnik, Hvar, Bakar and Cres (see locations in Fig. 1, some names are abbreviated). Since SST does not change rapidly in time, these measured values are compared to the analyses at 06, 12 and 18 UTC.

Several automatic stations on the eastern Adriatic coast measure SST on buoys anchored close to the coastline with an hourly interval (Zadar, Mljet, Malinska, Opatija, Dubrovnik and Crikvenica, see locations in Fig. 1). On stations Zadar, Dubrovnik and Opatija, there were both conventional and automatic measurements available.

There are operational SST measurements available for a number of stations in Italy from ISPRA (Italian National Institute for Environmental Protection and Research). The SST measurements from the stations in Italy are mostly available with an hourly interval.

2.2. Meteorological model

The operational forecast (Tudor et al., 2013) is used as the reference. The forecast suite consists of 8 km resolution forecast up to 72 h run twice per day from 00 and 12 UTC. The initial conditions for 8 km run are obtained from local data assimilation cycle where three-dimensional Variational (3D-Var) method is used for the analysis of the upper air fields while optimal interpolation method is used for analysis of surface fields (Stanešić, 2011). The second component of the operational forecast is 2 km resolution run up to 24 h run once per day. It stars at 06 UTC, using initial conditions interpolated from the 8 km resolution run without data assimilation.

2.2.1. Operational 8 km hydrostatic forecast using ALADIN system

The operational forecast is computed using ALADIN System. It is a spectral limited-area model (LAM) with a quadratic elliptic truncation (Haugen and Machenhauer, 1993) that ensures that the non-linear terms of the model equations are computed without aliasing. The domain in 8 km resolution consists of 240 × 216 grid points, including an unphysical band of 11 points along northern and eastern boundaries needed for the biperiodization (Fig. 2a). The model equations are solved using semi-implicit semi-Lagrangian discretization (Robert, 1982) and finite differences on 37 levels in the vertical with hybrid pressure type eta coordinate (Simmons and Burridge, 1981). This includes the stable extrapolation two time level, semi-implicit, semi-Lagrangian advection scheme (SETTLS, Hortal, 2002) with a second-order accurate treatment of the non-linear residual (Gospodinov et al., 2001). Semi-Lagrangian horizontal diffusion (SLHD) (Váňa et al., 2008) is based on the physical properties of the flow. The operational physics parametrisations at the time include prognostic TKE, cloud water and ice, rain and snow (Catry et al., 2007) and diagnostic scheme for deep convection (Geleyn et al., 1995). The model variables are coupled to a large scale model at the lateral boundaries using a relaxation scheme (Davies, 1976) in a zone, which is 8 grid points wide. The global model data are available with a 3-hourly coupling interval that could be insufficient to capture rapidly moving storms (Tudor and Termonia, 2010; Tudor, 2015). The initial conditions are computed by combining 3D-Var for the upper air fields and optimal interpolation for surface (Stanešić, 2011).

The operational package of physics parametrizations uses a simple microphysics scheme with prognostic cloud water and ice, rain and snow (Catry et al., 2007) with a statistical approach for sedimentation of precipitation (Geleyn et al., 2008). The ratio of evaporation and fall speed for liquid and solid precipitation is reduced (Tudor, 2013) to avoid excess precipitation as a consequence of fibrillations that arise due to stiffness. The operational radiation scheme (Geleyn et al., 2005a,b) is simple and computationally cheap using only one spectral band for computation of the long-wave and one for short-wave radiation. Prognostic TKE (Geleyn et al., 2006) scheme includes a contribution of the shallow convection (Geleyn, 1987). The exchange with surface (Noilhan and Planton, 1989) and the surface data assimilation (Giard and Bazile, 2000) use the Interaction Soil Biosphere Atmosphere (ISBA) surface scheme. The turbulent exchange at the sea surface uses different mixing lengths for momentum and heat (Brožkova et al., 2006) that are modified from Charnock (1955). The interpolation of wind, temperature and humidity from the lowest model level (about 17 m above ground) to the heights of the standard meteorological measurement (10 and 2 m above ground) is computed using a parametrized vertical profile dependent on stability (Geleyn, 1988).

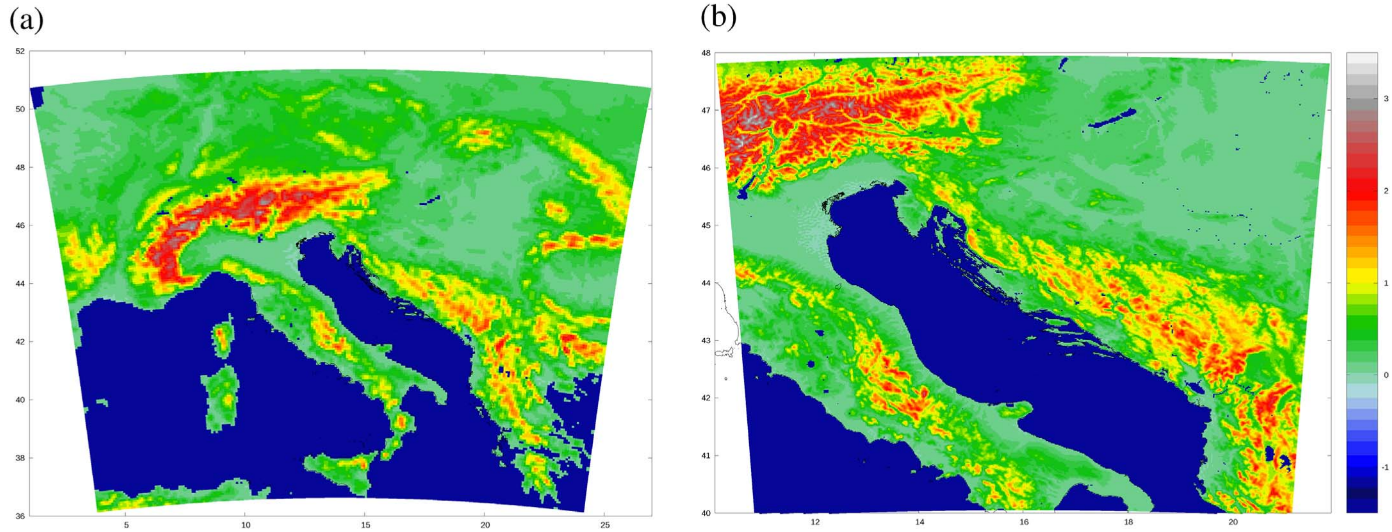

Fig. 2. Terrain height in model domains in 8 km (a) and 2 km (b) resolution.

2.2.2. Operational 2 km non-hydrostatic ALADIN forecast

A high resolution operational forecast run, uses ALADIN System with non-hydrostatic dynamics (Bénard et al., 2010) and a complete set of physics parametrizations, including the convection scheme (Tudor and Ivatek-Šahdan, 2010). The model domain is shown in Fig. 2b. The convection scheme is a prognostic one (Gerard and Geleyn, 2005; Gerard, 2007) and it allows combining resolved and convective contributions in the gray zone (Gerard et al., 2009). This forecast is computed using initial conditions interpolated from the 6 hour forecast of the 8 km resolution forecast that starts at 00 UTC. It is initialized using scale selective digital filter initialization (SSDFI, Termonia, 2008). It also uses hourly LBCs from the 8 km resolution forecast runs for 24 h, until 06 UTC on the next day. That allows comparison to precipitation data from the rain-gauges available in the high resolution network.

The 2 km resolution simulations are often regarded as explicitly resolving convection and this implies that there is no parametrization of convection used (Lebeaupin et al., 2006). The shortest wave represented by the model dynamics in the quadratic truncation in 2 km resolution is actually $3\Delta x$ or 6 km in wavelength. Therefore, we use the 3MT convection scheme to parametrize the unresolved portion of deep convection. The model and domain characteristics are summarized in Table 1.

2.2.3. Precipitation data

The observational precipitation data used here are from the network of stations that operate routine meteorological measurements in Croatia and those from abroad that are available through routine international exchange. In 2012 the Croatian rain-gauge network consisted of more than 500 stations reporting accumulated rainfall for the 24 h from 06 UTC until the 06 UTC the next day. The precipitation data from SYNOP reports is used for other countries in the domain.

However, insitu data do not tell us much about the precipitation over the sea. In order to fill in this void, precipitation estimates from satellite data are used. Satellite derived precipitation data are used as provided from the Tropical Rainfall Measuring Mission (TRMM, Huffman et al., 2007), in particular we use the 3-hourly precipitation data from 3B42RT product and computed 24-hourly accumulated rainfall for the period from 06 UTC to 06 UTC the next day. The TRMM data are available from Giovanni web server interface (Acker and Leptoukh, 2007) on http://disc.sci.gsfc.nasa.gov. These data were used to subjectively evaluate the spatial distribution of precipitation, but not in the computations of statistical scores.

Table 1
Summary of ALADIN System characteristics used in operational model set up in autumn 2012.

Resolution	8 km	2 km
Discretization	Spectral, quadratic truncation, A grid, 37 hybrid levels	
Size	240 × 216 gridpoints	450 × 450 gridpoints
See	Fig. 2a	Fig. 2b
Dynamics	Semi-implicit, semi-lagrangian advection, SLHD	
	hydrostatic	nonhydrostatic
Physics	TKE, prognostic microphysics, radiation (Geleyn et al., 2005a,b)	
Convection	Diagnostic	Prognostic (Gerard et al., 2009)
Initialization	3D-Var	SSDFI
Surface	ISBA soil scheme, SST from global model used for LBCs	

2.3. SST computations

The model has one field that describes the surface temperature (regardless the underlying surface) and another field that represents land sea mask (LSM), which can assume only two values: zero for sea/water surface and one for land. In the subsequent computations, surface temperature in the model is modified only for grid points where LSM is zero (sea points).

2.3.1. Introducing OSTIA and MUR SST analyses to ALADIN model fields

For each ALADIN model grid point with LSM equal to zero, one would look for the closest sea point in the OSTIA or MUR analysis of SST. If this point in the analysis is closer than a predefined distance, the SST value from the analysis is used. If the closest point in the analysis is too far, the original operational value is kept, preventing the procedure from modifying data on lakes.

This approach works fine for MUR analysis of SST that is in high resolution and has data over the southern portion of the Velebit Channel (VC). When introducing OSTIA SST analysis, this approach does not modify SST in the southern part of VC unless it also modifies SST over the Skadar Lake (Figs. 3b and 4b). The OSTIA SST analysis does not contain SST data over the southern VC. To make things worse, the closest sea point for the southernmost portion of VC is Zadar (in the south), not the northern part of VC.

While developing the procedure, an experiment forecast was done in which the procedure for incorporating OSTIA SST was modified so that southern part of VC uses SST from the northern part (from the sea it is connected to) and not from the closest area (close to Zadar). This yields constant temperature over southern VC that has the same value as the closest point in OSTIA.

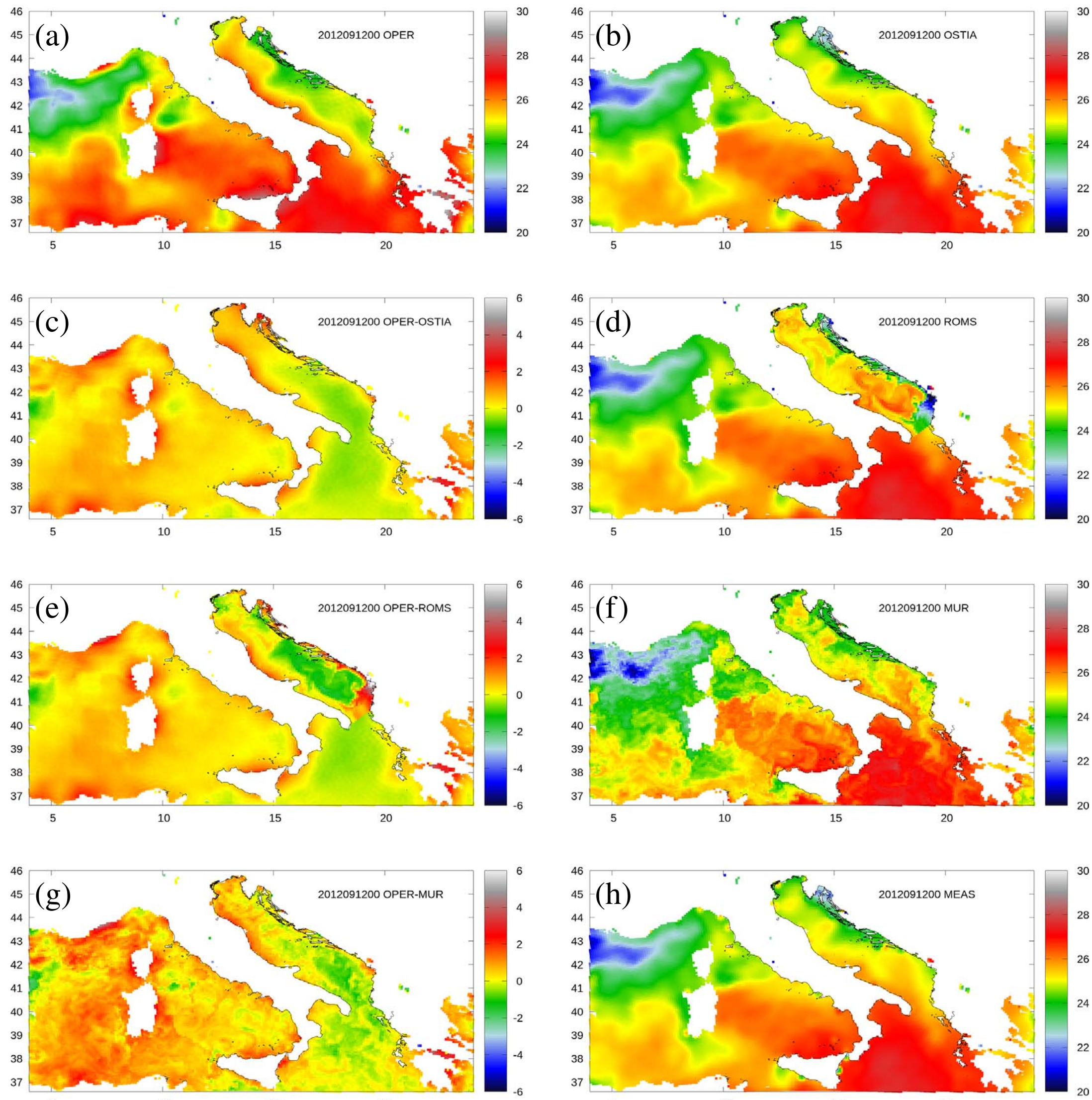

Fig. 3. SST (°C) from the operational run in 8 km resolution (a), when OSTIA analysis is inserted (b), difference OPER-OSTIA (c), when ROMS is inserted in the field already modified by OSTIA (d), difference OPER-ROMS (e), when MUR analysis is inserted (f), difference OPER - MUR (g) and OSTIA inserted and nudged towards in situ measurements (h) for 00 UTC 12 September 2012.

2.3.2. Introducing ROMS model data to ALADIN model fields

The ROMS domain covers only Adriatic. Consequently, ROMS data are inserted in the SST field that is already modified by values from OSTIA analysis (Figs. 3d and 4d). The ROMS model SST data are used in the model so that for each ALADIN model grid point with LSM equal to zero, one would look for the closest point in the ROMS field and assign a value to the model SST that is computed as:

$$T_n = T_m + \frac{r_M - r_d}{r_M}(T_r - T_m) \tag{1}$$

where T_n is the new SST value, r_M is maximum radius of influence (tuning parameter that can smooth the transition at the edge of ROMS domain), r_d is the distance between the ALADIN and ROMS grid-points, T_r is SST from the closest point in ROMS and T_m is the ALADIN model SST in a grid point (already modified by OSTIA data). The above formula therefore uses the closest sea point on the ROMS grid. The same procedure can be used to smooth the transition of SST at Otranto Strait from ROMS to OSTIA data. Otherwise, there could be sharp artificial gradients. $r_M = 0.25°$ is used in the experiments shown here.

The MUR SST data have been introduced using the same approach but over the whole domain. The data coverage is global and without problems in the Velebit Channel, since MUR analysis has the data there (Figs. 3f and 4f).

2.3.3. Introducing in situ measurements of SST

As mentioned in the introduction, it was suggested that introducing insitu measurements into the SST field could improve the precipitation forecast. One experiment tests this hypothesis for the HyMeX SOP1 period. The SST field, modified by values from OSTIA analysis, is nudged towards SST values measured insitu. For each ALADIN model grid point with LSM equal to zero, one computes the distance to the closest point of measurement r_s. If this distance is less than a predefined value r_M, the new SST value is computed as

$$T_n = T_m + \frac{r_M - r_s}{r_M}(T_s - T_m) \tag{2}$$

where T_n is the new SST value, r_M is maximum radius of influence (tuning parameter that defines the area of influence of the point measurement), r_s is the distance between the ALADIN grid-point and the point of measurement, T_s is the measured SST from the closest station and T_m is the ALADIN model SST in a grid point. The above formula is applied only for the closest point of measurement and only if it is closer than $r_M = 0.5°$. The resulting fields are illustrated in Figs. 3h and 4g.

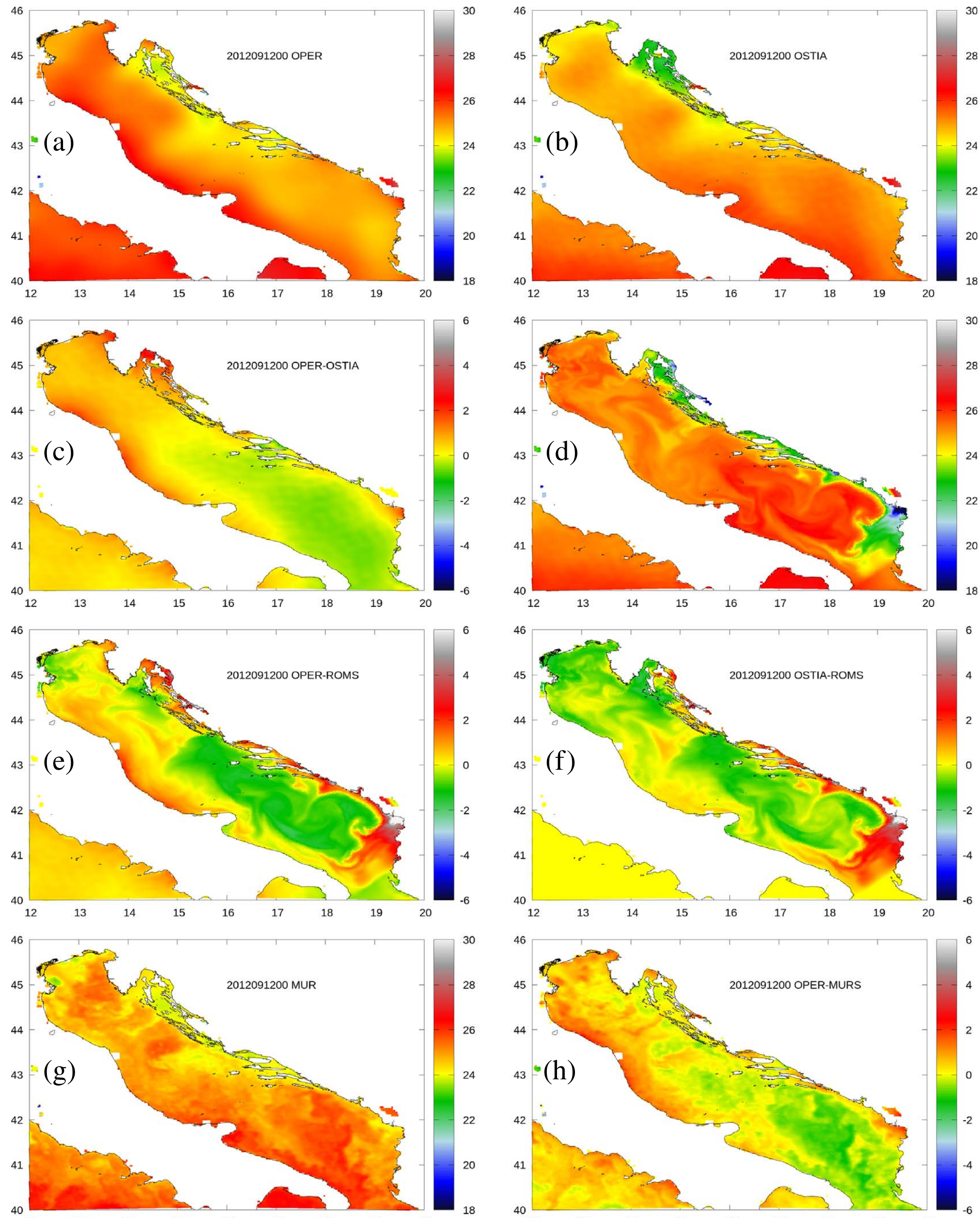

Fig. 4. SST (°C) from the operational run in 2 km resolution (a), when OSTIA analysis is inserted (b), difference OPER-OSTIA (c), when ROMS is inserted in the field already modified by OSTIA (d), difference OPER-ROMS (e), and OSTIA-ROMS (f), when MUR analysis is inserted (g), difference OPER - MUR (h) for 00 UTC 12 September 2012.

2.4. The intensive precipitation event in Rijeka during IOP2 in the evening of 12 September 2012

The effect of SST on IPEs is tested on the whole SOP1 period and on one particular intensive observation period (IOP) during SOP1. During SOP1 several IOPs were declared. During IOP2, a heavy precipitation event occurred over the north-eastern Italy, Slovenia and north-west Croatia in the afternoon and evening of 12 September 2012 (Manzato et al., 2015; Ivančan-Picek et al., 2016). The event is associated to the interaction of a warm and moist low level air-mass arriving from the Adriatic Sea and a cold front. During the day, there were three storms, several hours apart, over north-east Italy including a supercell storm that developed in the morning (Manzato et al., 2015) over north-eastern Italy. Nearby area of Istria and Rijeka received the first rainfall in the early afternoon, but precipitation stopped soon. Later in the evening, IPE occurred over north-west Croatia, particularly the city of Rijeka and surrounding area where several rain gauges measured more than 200 mm of precipitation in 24 h. According to the rain gauge in Rijeka, the torrential rain in the evening fell during 2 h between 21 and 23 UTC. It was connected to the last storm over Italy (Manzato et al., 2015) that was moving along the coast of north Adriatic over Istria towards Rijeka and Kvarner. During the day, moist air over the central Adriatic became saturated. Convection developed over the northern Adriatic and warm and moist advection produced intensive precipitation triggered by the orography. The flash floods occurred during the night and caused substantial damage.

Table 2
List of experiments for both 8 km and 2 km resolution.

Experiment	Description
OPER	Operational SST from ARPEGE
TM5K	SST reduced by 5 °C
TM2K	SST reduced by 2 °C
TP2K	SST increased by 2 °C
TP5K	SST increased by 5 °C
TM10	SST reduced by 10 °C
OSTIA	SST taken from OSTIA
ROMS	SST from ROMS over Adriatic and OSTIA elsewhere
MUR	SST taken from MUR
MEAS	SST from OSTIA nudged towards measurements

This IPE event was predicted by ALADIN operational forecasts in both 8 and 2 km resolution with precipitation exceeding 100 mm inland of Rijeka, but still underestimated 220 mm that was actually measured. This event is studied in more detail in Ivančan-Picek et al. (2016). Here we show that the position of maximum precipitation in the operational forecast was shifted inland from Rijeka due to too warm SST in Kvarner and Rijeka Bay and VC.

3. Results

In this section we first analyze the SST fields obtained by the procedure described above and used in subsequent experiments. The fields are illustrated in Figs. 3 and 4 for one day, 12 September 2012 to show how the spatial variability changes. Then, we compare the SST measured insitu to the values of SST fields in the closest sea point in the model used in different experiments for the whole SOP1 period. Afterwards, the precipitation forecasts from different experiments are evaluated. The experiments consisted of running 61 forecasts for up to 72 h in 8 km resolution and 61 forecasts up to 24 h in 2 km resolution. In each experiment SST was modified as explained in Table 2 and previous section. The results of experiments in 8 km and 2 km resolution are here discussed and illustrated for one case of IPE in Rijeka on 12 September 2012.

3.1. Qualitative evaluation of SST fields

In 2012, the data in the coupling files of ARPEGE was in 10.6 km resolution. The SST value in the initial file of the 8 km resolution forecast is modified using SST from different sources as described in the Subsection 2.3.

We compare the SST fields for one day during HyMeX SOP1 first, as an example of differences found on daily basis. Some inconsistencies in SST provided in the files could be attributed to low resolution of the global analyses and/or vicinity of the coastline. The operational SST taken from ARPEGE for 12 September 2012 (Fig. 3a) shows a cold pool (20–22 °C) spreading from the Bay of Lyon, a warm pool (28–29 °C) around Sicily and in Ionian Sea, while the rest, including Adriatic, is in the range from 24 °C to 27 °C. The SST is particularly warm in a narrow area close to Cotě d' Azur and SST field is rather warm and smooth over the Adriatic (24–26 °C). The SST used operationally is colder by 1–2 °C than any alternative SST for southern Adriatic and Ionian Sea.

On the other hand, SST from OSTIA analysis is colder over most of the Western Mediterranean and Aegean Sea (Fig. 3b and c) by 1 to 3 °C with an exception of the Ionian Sea, the central part in the southern Adriatic and few spots in the western Mediterranean. There is a cold pool in north-east Adriatic. The cold pool spreading from the Gulf of Lyon is few degrees colder than in ARPEGE and there is no warm belt along the Cotě d' Azur. The SST field from OSTIA has larger spatial variability with several cold pools.

The ROMS model output is available for the Adriatic and used to modify SST, which is already modified by OSTIA. The resulting SST field has high spatial variability over the Adriatic with large spatial gradients (Figs. 3, 4d and e). The SST is colder along eastern coastline, particularly between Istria and Velebit mountain and in south-east Adriatic close to the outlet of Bojana river, and slightly colder in the area close to Venice. The ROMS SST is the highest (when compared to SST analyses) in the central parts of middle and southern Adriatic, away from the coastline. The ROMS is actually much warmer than OSTIA over most of the Adriatic region (except close to coast in the south-east) while the cold pool in the north-east is less spatially extensive with larger temperature in Kvarner Bay, but lower in VC and Rijeka Bay. However, ROMS also contains SST data over the southern VC that is considerably colder (several °C) than the surrounding sea.

The MUR analysis provides SST in the highest resolution and the procedure applied here does not apply smoothing to it. Resulting SST has higher spatial variability than the operational SST from ARPEGE and OSTIA analysis (Fig. 3f and g). Just as OSTIA, the SST from MUR is colder than operational ARPEGE with an exception of southern Adriatic and several patches over western Mediterranean and the warm tongue of SST along Cotě d' Azur is non-existent. The cold pool in north-east Adriatic is less intensive than in ROMS and less spatially extensive than in OSTIA. The southern part of VC is also warmer than in ROMS.

In 2 km resolution operational run that uses SST from ARPEGE, the SST has low spatial variability (Fig. 4). When SST from OSTIA is used, SST is much lower in coastal areas; Kvarner Bay, Trieste Bay etc. The SST in the southern part of VC is left unchanged with respect to the operational one. The differences in SST exceed 4 °C. The SST from ROMS has the highest spatial variability and coldest values in the southern part of VC and south-east Adriatic (between Montenegro and Albania). On the other hand, ROMS is the warmest over the open sea of central and southern Adriatic. The differences between OSTIA and ROMS are the largest on the eastern side of Adriatic where SST from ROMS is lower.

The Fig. 4d shows results for ROMS with large radius of influence when SST of Skadar Lake was also modified using values from the sea nearby. This is because the same procedure was used to smooth the transition from ROMS SST to OSTIA SST at the Otranto Strait. The ROMS SST fields show dynamical features of the Adriatic sea such as eddies and filaments and interchanging tongues of warm and cold sea and SST exhibits sharp gradients. Other SST fields used here are smoother. Operational and OSTIA SST are smoother due to resolution. MUR SST analysis is in higher spatial resolution than ROMS but the field is smoother and much warmer along the eastern Adriatic coastline than ROMS. All alternative SST fields have higher values than operational for central and southern Adriatic and lower values along coastlines.

All SST fields show colder SST along the eastern Adriatic than at the middle and the western side. This is a bit different situation than usually found. The eastern Adriatic current is bringing warm water from the Ionian Sea. While the western Adriatic current flows south-east and is usually colder than the rest of the Adriatic. The strong, cold and dry bura wind from the eastern shore can cool the sea surface by several degrees in a day. The sea evaporates intensively and looses heat due to latent heat consumption. Strong wind also enhances mixing of the sea in vertical.

3.1.1. Point-based comparison of SST to in situ measurements

Here we compare the model SST in the modified initial fields with the values measured on the stations. The operational SST used in the comparison is taken from the nearest sea point in the coupling file from ARPEGE. Since the coupling files contain data in 10.6 km resolution on a Lambert conformal grid, which is not native to the ARPEGE global model, there is already some horizontal interpolation involved when the files are created in Météo France and we want to avoid any additional interpolation. The SST in the forecast coupling files is the same as in the initial file. Therefore, the SST is taken only from the analysis fields of ARPEGE on 10.6 km resolution grid.

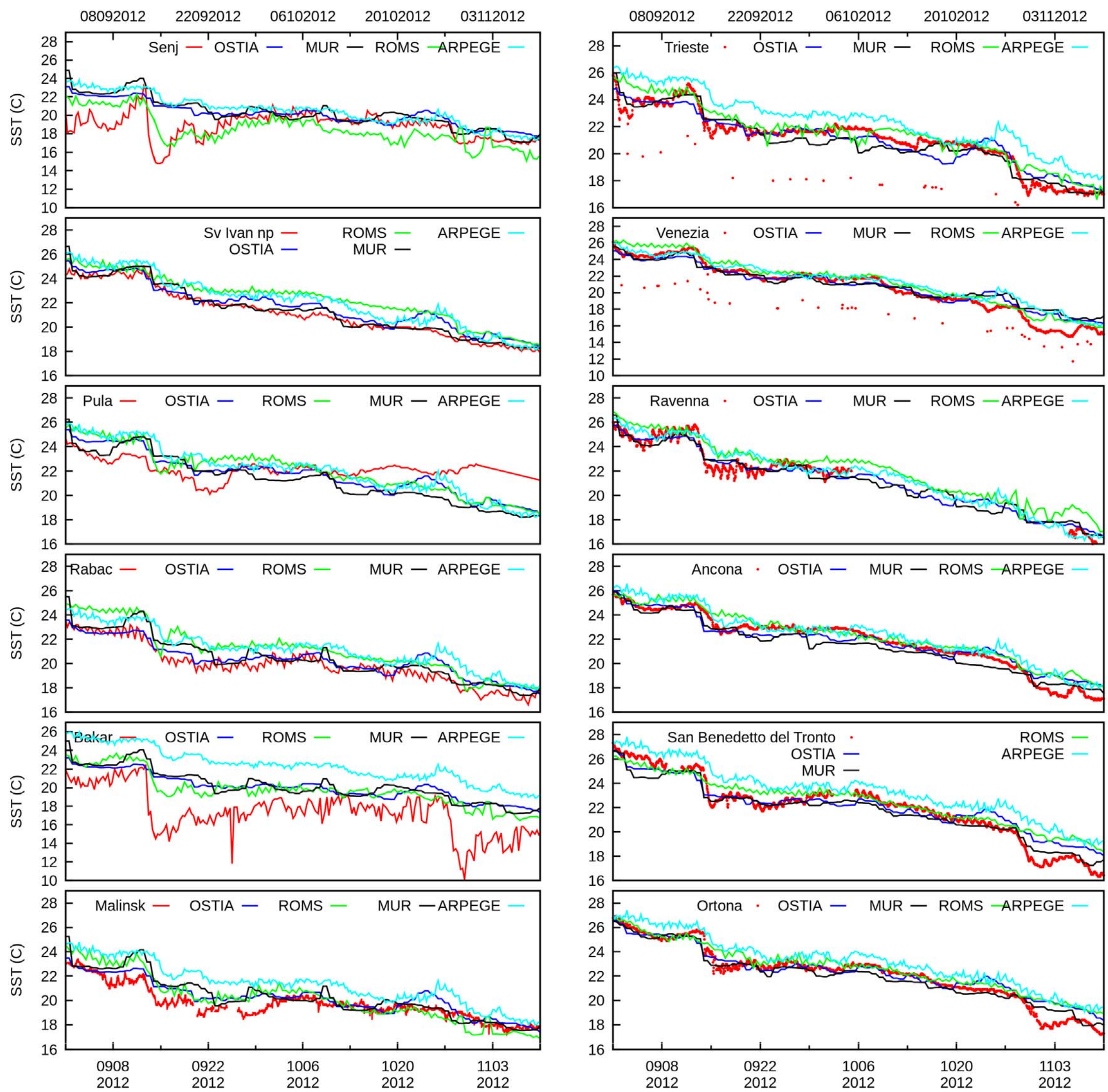

Fig. 5. SST measured on station (red), from ARPEGE coupling files (cyan), OSTIA (blue), ROMS (green) and MUR (black) coupling files for different stations for the period from 1 September to 10 November 2012. (For interpretation of the references to color in this figure legend, the reader is referred to the web version of this article.)

On the other hand, the SST from OSTIA and MUR analyses are introduced to the 8 km resolution initial fields that are on a Lambert conformal grid using a procedure described in Chapter 2. The SST data from ROMS and insitu measurements are used to modify the SST field that is already modified by OSTIA on the same 8 km resolution grid.

Unlike the ARPEGE, the SST data for OSTIA, MUR and ROMS, which are used in the comparison, are taken from the nearest sea point in the initial file of ALADIN on 8 km resolution grid. Since we simply overwrite the value of model SST by the values from OSTIA or MUR analyses (if the corresponding point is a sea point), there is no interpolation involved and the SST values are in fact equal to the closest sea point in the analyses.

The data from the nearest sea point is taken to evaluate the SST provided in the coupling files from ARPEGE for a number of stations where in-situ measurements of SST are available. The measured data are plotted against SST values from the nearest sea point for the period from 1 September to 10 November 2012 (Fig. 5). The measured data are not smoothed for the diurnal cycle of SST. The ARPEGE and ROMS data also have a diurnal cycle, while analyses have one daily value. We do not compute errors here, but try to identify when and where the differences between measured values and those from model/analyses are the largest. The Fig. 5 reveals several characteristics:

- On most stations, there is an agreement in temporal changes in SST on long time scales even for several stations with complex coastline and surrounded by islands unresolved in global models.
- Measured SST shows larger temporal variability than the analyses and models. The difference between measurements and reanalysis/model data is often lower than the amplitude of the diurnal cycle in SST.
- On Senj and Bakar stations, measured SST is lower and far more variable than in analyses, possibly due to local ocean dynamics and local atmospheric features, such as cold and dry bura wind, which rapidly cools the sea surface.
- The ROMS reproduces the cooling event on 12–14 September 2012, although it slightly underestimated the reduction of SST on both sides of Adriatic.
- The MUR and OSTIA reproduce the same cooling event on the western coastline (although slightly underestimated by OSTIA), underestimate the cooling at Trieste, but there is only a hint of the cooling at Senj and Bakar on the eastern Adriatic coastline.

Although we compare SST fields from the closest sea point and in-situ measurements that are done on the coastline, there is a good agreement in measured and model SST for the most of the stations.

The SST changes on a scale of several weeks are represented in

ARPEGE. Local events with rapid cooling (such as for Senj and Bakar on 12 September 2012, Fig. 5) are not represented in the changes in the SST provided from ARPEGE, and for several locations these cooling events are underestimated by the analyses. Measurements of SST on several stations exhibit similar intensive variations that are not present in SST data from analyses but these changes are represented in the ROMS model output.

The comparison of measured and operationally used SST reveals a significant bias. These differences can be substantial, especially in Rijeka Bay and VC (see stations Senj, Bakar, Rabac and Malinska in Fig. 5). These areas are much colder than the rest of the Adriatic sea during HyMeX SOP1. This is not resolved in the SST fields from ARPEGE and OSTIA, while MUR analysis is warmer than insitu measurements. The area is small and contains many islands close to the coastline. It is not surprising that the cold pool is missed in the SST fields presented with the resolution of the global NWP model. This cold area has an impact on the local weather and on the meteorological parameters measured on the coastline, especially 2 m temperature and humidity. Using SST from a high resolution analysis or ocean model forecast, where these islands are resolved and well represented, could have a positive impact on the overall forecast performance. However, the comparison to measurements reveals that the cold pool between Istria and Velebit mountain is actually better represented in OSTIA than in MUR analysis.

The SST fields from ARPEGE do show that sea surface is slightly colder close to the Italian coast of Adriatic than at the open sea, but insitu measurements show much colder sea surface there. This cold area is probably too narrow to be resolved by the global model ARPEGE and therefore colder Western Adriatic Current (WAC) is not present. It is possible that there are other high-resolution features in SST that are not well represented in the data used by the global NWP models. This cold sea current considerably affects 2 m temperature and humidity measured on meteorological stations nearby, which in turn could be rejected in the subsequent procedure for data assimilation.

3.2. Impact of changes in the SST on precipitation forecast

The impact of SST on the intensity and location of intensive rainfall is investigated. The operational run at the time of HyMeX SOP1 is driven by ARPEGE forecasts as lateral boundary conditions and SST is taken from the initial file of ARPEGE. In the first set of experiments, SST effects on forecast precipitation are analyzed by modifying the SST field in the initial file by shifting the SST field uniformly. For each model forecast, the initial SST field is modified by increasing or decreasing SST values by 2 °C and 5 °C and finally decreasing by 10 °C for all sea points in the model domain (see Table 2 for the list of experiments). These values are chosen on the basis of evaluation of model and analyzed SST against insitu data since the differences between measured and model SST reach and even exceed these values on several stations.

Precipitation accumulated over 61 days (Fig. 6a) from rain gauge measurements is lower than the TRMM estimate (Fig. 6b). The accumulated precipitation during 61 days of SOP1 from rain gauge measurements (Fig. 6a) shows a maximum extending from Kvarner bay to the Alps on the border between Austria, Italy and Slovenia. However, these measurements are done only over land and can be relatively sparse there, with vast areas of no data. The precipitation accumulated from the TRMM estimate for the same period (Fig. 6b) shows a secondary maximum over the southeast Adriatic, over the Montenegro coast, as well as over Ionian Sea. The latter shows several local maxima over the sea surface that are not present in the rain gauge data (because of the absence of insitu measurements there). Here we can not determine if TRMM overestimates or the rain gauges underestimate precipitation (or both!), especially for the wide areas with no measurements (such as the sea surface). The TRMM data represent precipitation activity at a resolution of 0.25°, which is coarser than the NWP models runs employed here. The rain gauge data are known to underestimate the precipitation amounts due to high wind. The precipitation amounts from rain gauges are not corrected for this effect (due to absence of measured wind speed at the location of almost all the rain-gauges).

3.3. Results of experiments with uniform shift of SST

Here we analyze the rainfall produced by experiments when the operational SST (from ARPEGE) is increased or reduced by a fixed number. The analysis of the 8 km resolution experiments is performed for the first day (precipitation accumulated from 06 to 30 h forecast) and the second day (from 30 to 54 h forecast). All experiments in 8 km resolution start from the 00 UTC analysis and only SST is modified. The precipitation from the first 6 h of the forecast is omitted from the analysis. The experiments in 2 km resolution start from the 06 h forecast of the corresponding experiment in 8 km resolution.

3.3.1. Precipitation in 8 km resolution

The precipitation accumulated during 61 days of SOP1 from ALADIN forecasts in 8 km resolution shows abundant precipitation along the eastern Adriatic, especially over the inland mountains (Fig. 7). Most of this precipitation is resolved with peaks of resolved precipitation over mountains. Convective precipitation is less intensive with intensity peak over the coastline and the sea surface. Over land, stratiform precipitation is more intensive than the convective precipitation, while the opposite can be said for the sea surface, where convective precipitation dominates.

The forecast precipitation peaks are located over mountain peaks and ridges, where no in situ measurements are available, but these precipitation amounts can be seen in the TRMM data (Fig. 6b). The operational precipitation maxima over the sea surface (Fig. 7) are much lower than the values from TRMM data, especially over the Tyrhennian Sea. It requires a substantial increase in the SST to reproduce that amount of precipitation by the model, since only TP5K experiment reaches the amount given by TRMM (Fig. 7b).

Increasing/decreasing the SST produces more/less precipitation over the sea surface for all experiments with uniform shift in SST (for the difference with TP5K see Fig. 7). The increase is more pronounced in the output of the convective scheme (unresolved precipitation) than the stratiform (resolved) precipitation. Precipitation is also larger over the most of the surrounding mountains (Apennines and Dinaric Alps). There is one exception. The Alpine slopes of the Po valley receive more precipitation when SST is lower (Fig. 8). This enhanced precipitation is mostly from the stratiform (resolved) precipitation scheme (Fig. 8). Both convective and stratiform schemes yield more rainfall on the northern slopes of the Po valley when SST is lower. It is expected to get less precipitation overall with lower SST because the colder sea surface evaporates less. The colder sea surface triggers less convection over the sea surface, therefore more moisture reaches the Alpine slopes. Consequently, precipitation can be convective or stratiform, triggered by warm land surface, convergence of moisture by mountain flow or forced lifting upslope.

Operational SST over Ionian Sea is lower than OSTIA and MUR analyses. Warm SST evaporates more and more convection is triggered. The TRMM data show intense precipitation over Ionian Sea that is absent from the operational forecast. The reason could be low SST there. However, another precipitation peak in TRMM data, over the Tyrhennian Sea, is also underestimated by the operational forecast. But the operational SST there is higher than in the analyses, therefore underprediction of precipitation there could not be explained by too low SST. The forecasts, on the other hand, overpredict precipitation over the slopes of the surrounding mountains. This suggests that the precipitation is not triggered over the sea surface, but only when the moist air is forced upslope. Similar effect can be observed for the eastern Adriatic, where the precipitation maxima in TRMM (Fig. 6b) data is spread over the sea surface further than in the model forecast (Fig. 7a). However, precipitation data measured insitu (Fig. 6a) suggest that

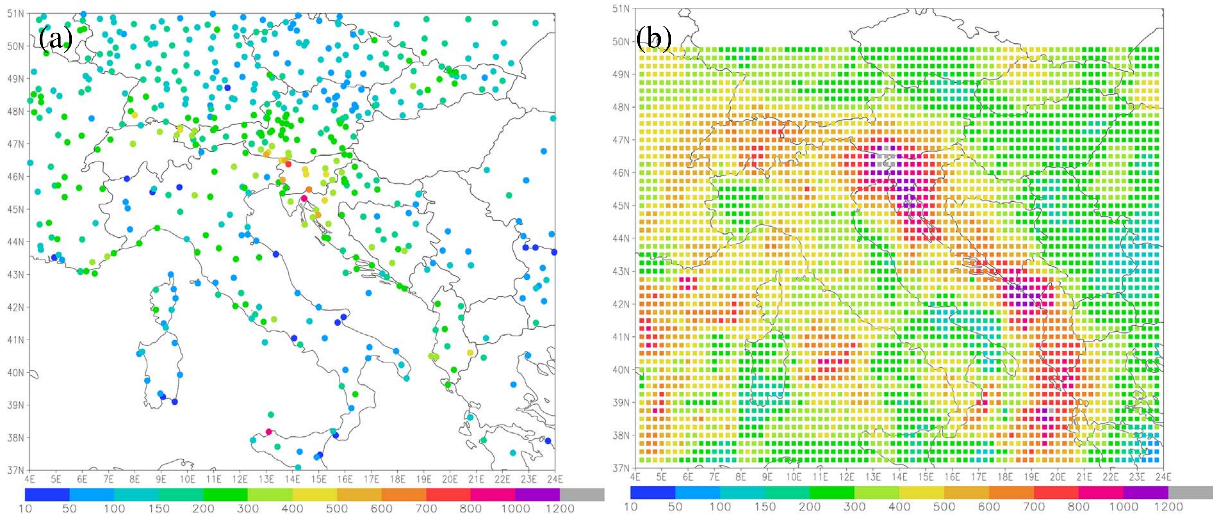

Fig. 6. Precipitation (mm) accumulated during 61 days of SOP1 measured on SINOP stations (a) and TRMM estimate (b). TRMM values are plotted as a small square at the point where data is available.

TRMM might exaggerate the precipitation amount over the eastern Adriatic coastline and islands. The convective precipitation was triggered above the sea surface even when SST was reduced by 10 °C (experiment TM10, figure not shown).

3.3.2. Precipitation in 2 km resolution

The 2 km resolution forecast produces higher precipitation maxima than 8 km forecast over the mountains along the eastern Adriatic (Fig. 9). The mountain peaks and ridges are higher in increased horizontal resolution and the slopes are steeper. Most of this enhanced precipitation intensity arises from the convection scheme (Fig. 9e and f), especially for the seaward slope of the mountains. The local maximum of resolved precipitation is over the ridge of the Velebit mountain (Fig. 9c), while the maximum intensity of the convective precipitation is on the slope facing the sea (VC, Fig. 9e). There is also more convective than stratiform precipitation over the sea surface (Fig. 9c and e).

Comparing the precipitation forecasts in TM5K and TP5K experiments (with decreased and increased SST) shows that when SST is lower the precipitation decreases over most of the domain, with an exception of southern Alpine slopes and an area between Ortona and Ancona (Fig. 9b). Both resolved and convective precipitation increase on the southern slopes of Alps (north of Po valley) (Fig. 9d and f). As already mentioned (in the 8 km resolution experiments discussion) lower SST triggers less convective precipitation over the sea surface, therefore, more is left to precipitate over the Alpine slope. Lower SST slightly increases precipitation in the area between Ancona and Ortona in Italy due to enhanced resolved precipitation (Fig. 9d) and little change in the convective precipitation. There is similar effect in 8 km resolution forecast (Fig. 7c). When SST is reduced, the precipitation over Velebit mountain shifts from convective to stratiform (Fig. 9d and f). Consequently, there is more stratiform precipitation over Velebit in TM5K experiment than in TP5K experiment (Fig. 9d). The stratiform precipitation is enhanced but the convective is reduced even more, consequently the overall effect of reducing SST on the precipitation amount is negative on that location (Fig. 9b).

Operational SST is very smooth and misses several high resolution features. It contains errors that are not uniform in space. Shifting SST by a fixed value keeps the horizontal gradients of SST unaltered. On the other hand, the gradient between sea and land surface temperature did change substantially. The gradients in SST used operationally are lower than in fields from SST analysis and the ocean model.

The cold sea surface evaporates less, therefore less moisture enters the atmosphere. Therefore, it is expected to have less precipitation when the sea surface is colder. When the sea surface is warmer, evaporation is more intensive and the atmosphere receives more moisture, the atmosphere produces convection and more precipitation is triggered over the sea surface. On the other hand, more stable (but still moist) air does not precipitate (as much) over the sea surface, but carries the moisture over the valley towards the Alpine slopes. The stable air is forced upslope and precipitates mostly through the resolved upward motions or triggered by moisture convergence. In TM5K experiment, cold but moist air moves from colder sea surface to warmer land surface. More precipitation is triggered when this moist air is forced upslope and not over the flat Po valley before the mountain.

3.4. Results of experiments with SST from analyses and ROMS

Here we analyze the precipitation in experiments where operational SST is replaced by SST from OSTIA, MUR and ROMS. As for the uniform shift experiments, we compare the results accumulated during 61 days of HyMeX SOP1 of the 24 hourly precipitation. All experiments start from the same analysis with modified SST.

3.4.1. Precipitation in 8 km resolution

There is more precipitation in the operational forecast (Fig. 8b) than in any of the experiments (OSTIA, ROMS, MUR) over western Mediterranean (10–50 mm over 61 days) due to increase in convective precipitation (Fig. 8d and f) with negligible differences in results between the experiments (results are shown only for the ROMS experiment).

The operational forecast used warmer SST there which in turn enhanced convection over warmer sea surface. Consequently, there is more convective precipitation in OPER (Fig. 8f). However, OPER has slightly more rain over lateral parts of Ionian Sea (Fig. 8b) where SST is lower than in other experiments, probably due to advection of moisture from neighboring areas (warmer seas). Over Adriatic and Otranto, there are interchanging areas of positive and negative precipitation differences (positive means OPER yields more precipitation). That suggests a shift of precipitation northward (downstream for most of the precipitation cases here) in the Otranto Straight in OPER with respect to OSTIA and westward (and from land to the sea surface) in MUR. In both experiments, SST is lower in OPER.

Precipitation in the southeast Adriatic decreases more in the ROMS experiment due to existence of a cold pool of SST in that area during part of SOP1. However, OPER yields less precipitation over central and

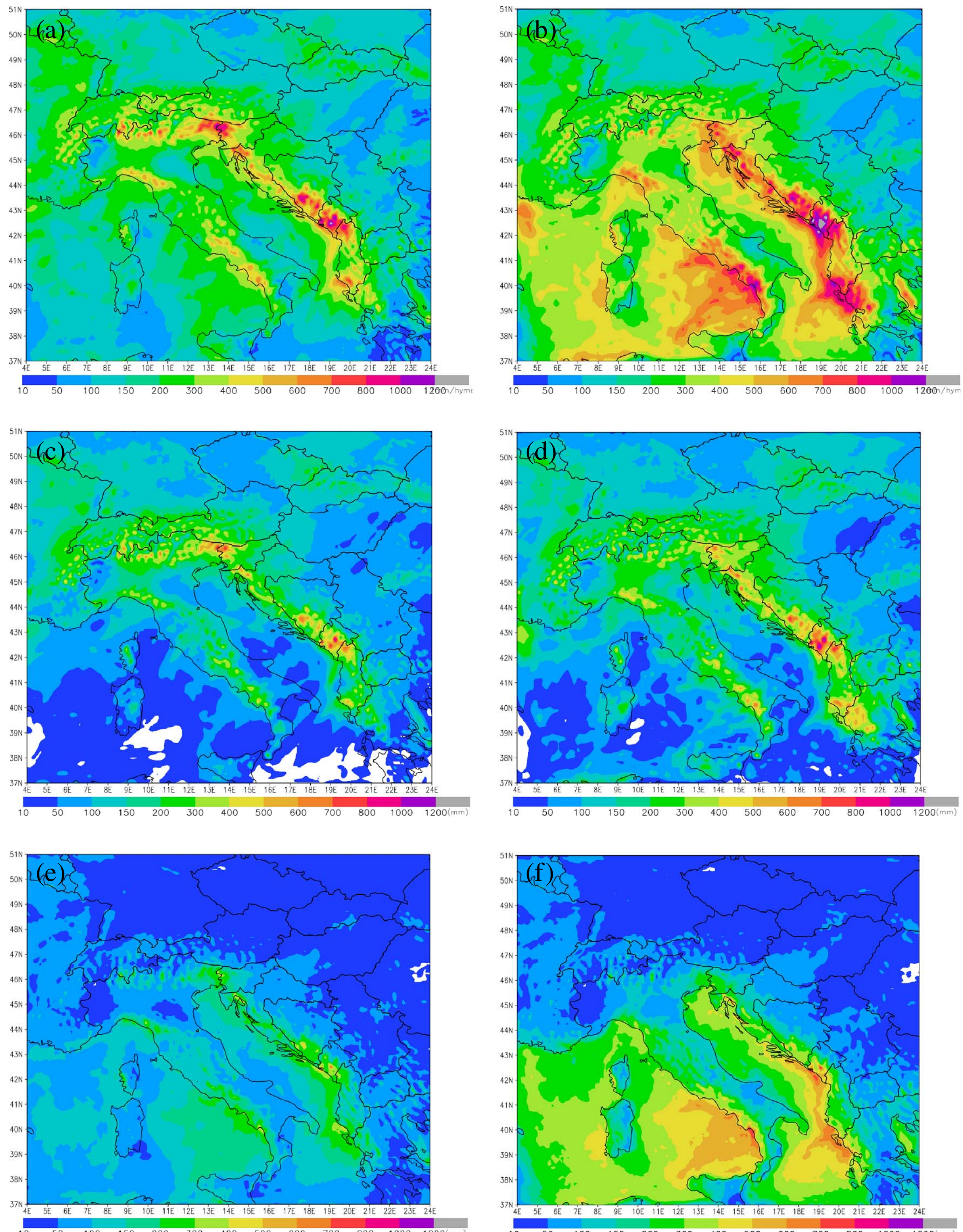

Fig. 7. Precipitation (mm) accumulated during 61 days of SOP1 from 8 km resolution forecasts initiated at 00 UTC and accumulated from 06 to 30 h of forecast: total (a, b), resolved (c, d) and convective (e, f) from operational forecast (a, c, e) and experiment TP5K (b, d, f).

southern Adriatic than ROMS (Fig. 8b) with less pronounced differences for OSTIA and MUR (not shown). Both resolved and convective precipitation are less intensive in the OPER experiment than in ROMS experiment there (Fig. 8d and f). The SST over most of the central and southern Adriatic (away from coastlines) is substantially warmer in ROMS (Fig. 3d and e). This enhanced evaporation, triggered more precipitation above the sea surface and also brought more moisture to the coastal areas to the north.

Most of the Northern Adriatic receives more rainfall in the OPER experiment, especially the area of Kvarner, where the differences in SST are also the largest (Fig. 8b). However, the most northwest part, around Venice and stretching inland, actually receives less precipitation in the OPER experiment, although SST there is also higher (in OPER than in other experiments). The differences in convective precipitation are mostly limited to the sea surface and nearby mountains (Fig. 8f).

The impact of SST on the stratiform precipitation reaches further inland, especially for the area east of the Adriatic coast (Fig. 8d). The influence of SST spreads more than 200 km from the shore although

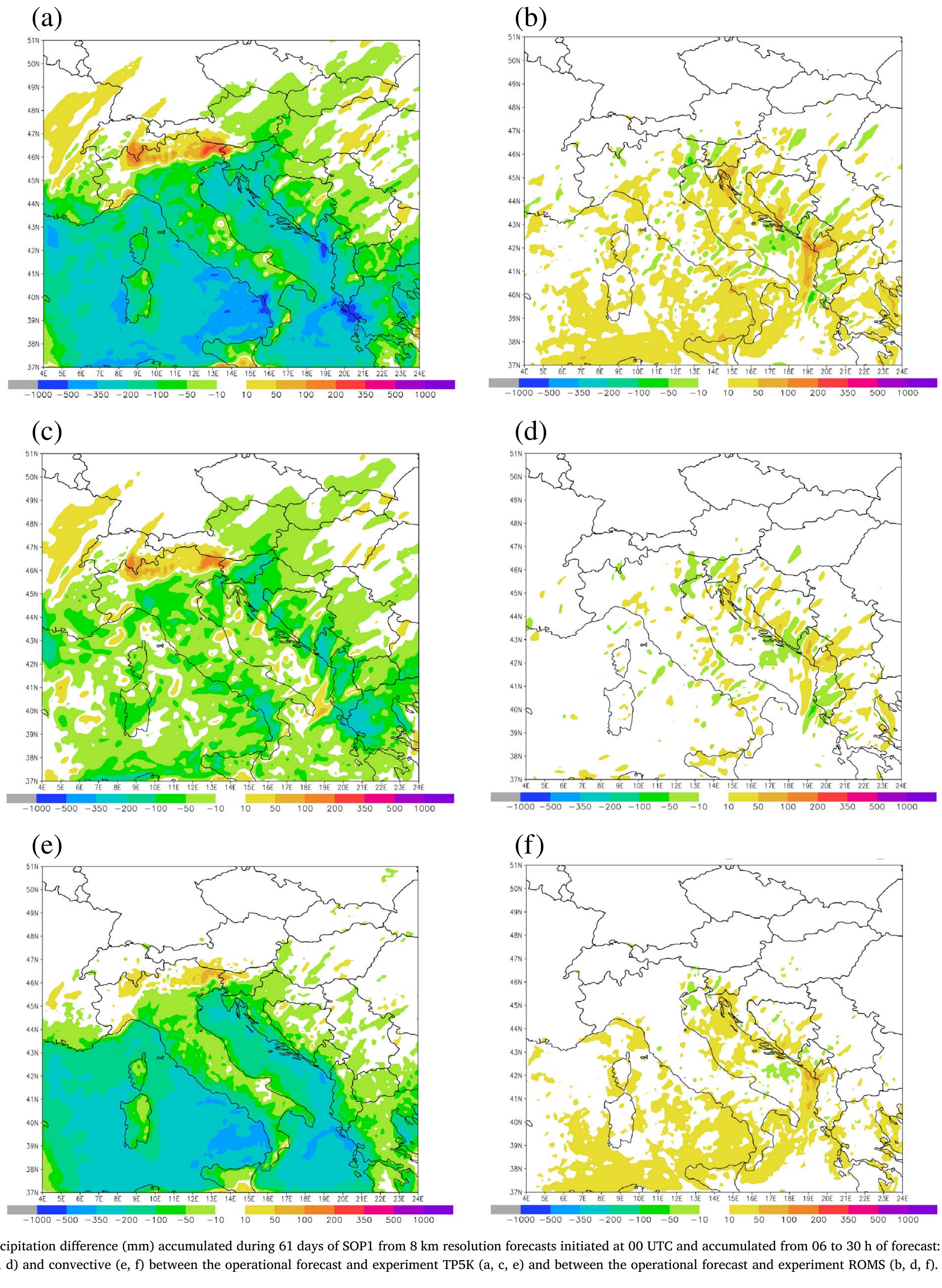

Fig. 8. Precipitation difference (mm) accumulated during 61 days of SOP1 from 8 km resolution forecasts initiated at 00 UTC and accumulated from 06 to 30 h of forecast: total (a, b), resolved (c, d) and convective (e, f) between the operational forecast and experiment TP5K (a, c, e) and between the operational forecast and experiment ROMS (b, d, f).

there are many mountains on the way.

3.4.2. Precipitation in 2 km resolution

The precipitation from different experiments is accumulated during 61 days of HyMeX SOP1 and its differences with respect to the reference are shown in Fig. 10 (positive values of reference minus experiment mean more precipitation in the reference run and negative values mean more precipitation in the experiment). The local intensity of precipitation can be substantially different, exceeding 200 mm (both negative and positive values in Fig. 10). However, an area with positive

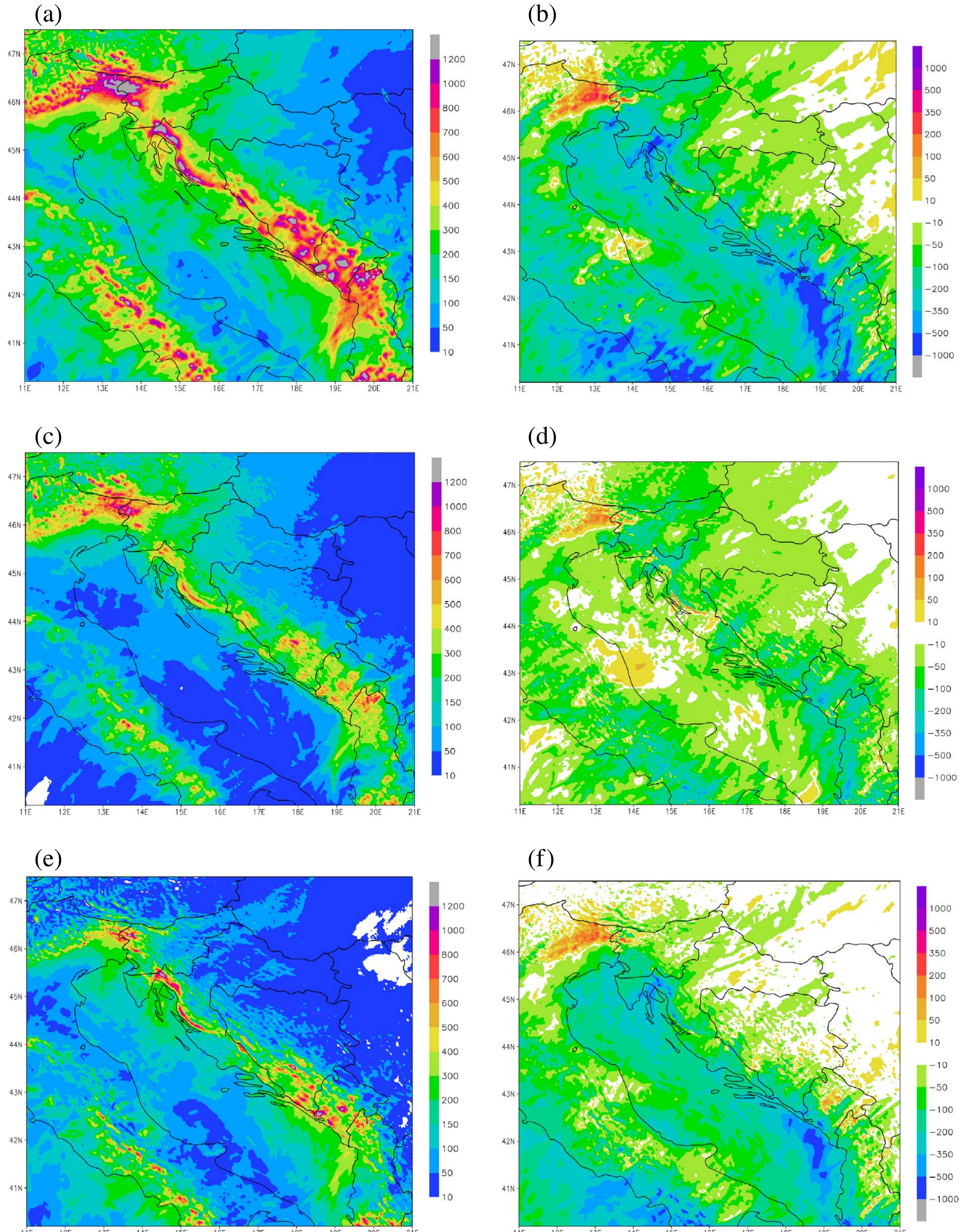

Fig. 9. Precipitation (mm) accumulated during 61 days of SOP1 from 2 km resolution forecasts: total (a, b), resolved (c, d) and convective (e, f) from reference forecasts (a, c, e) and difference between the TM5K and TP5K experiments (b, d, f).

precipitation difference is usually adjacent to an area with a negative difference. This means that precipitation has slightly shifted. The exceptions are an area stretching southward of Rijeka over Mali Lošinj island and southeastern Adriatic where reference yields substantially more precipitation due to warm SST. The precipitation for Dubrovnik increased in all experiments with respect to OPER (Fig. 10b, d, and f). The impact of SST change on convective precipitation reaches further inland than for 8 km resolution forecast because the 2 km forecast uses a prognostic convection scheme. Precipitation forecast in 2 km resolution is more sensitive to SST than the 8 km resolution forecast.

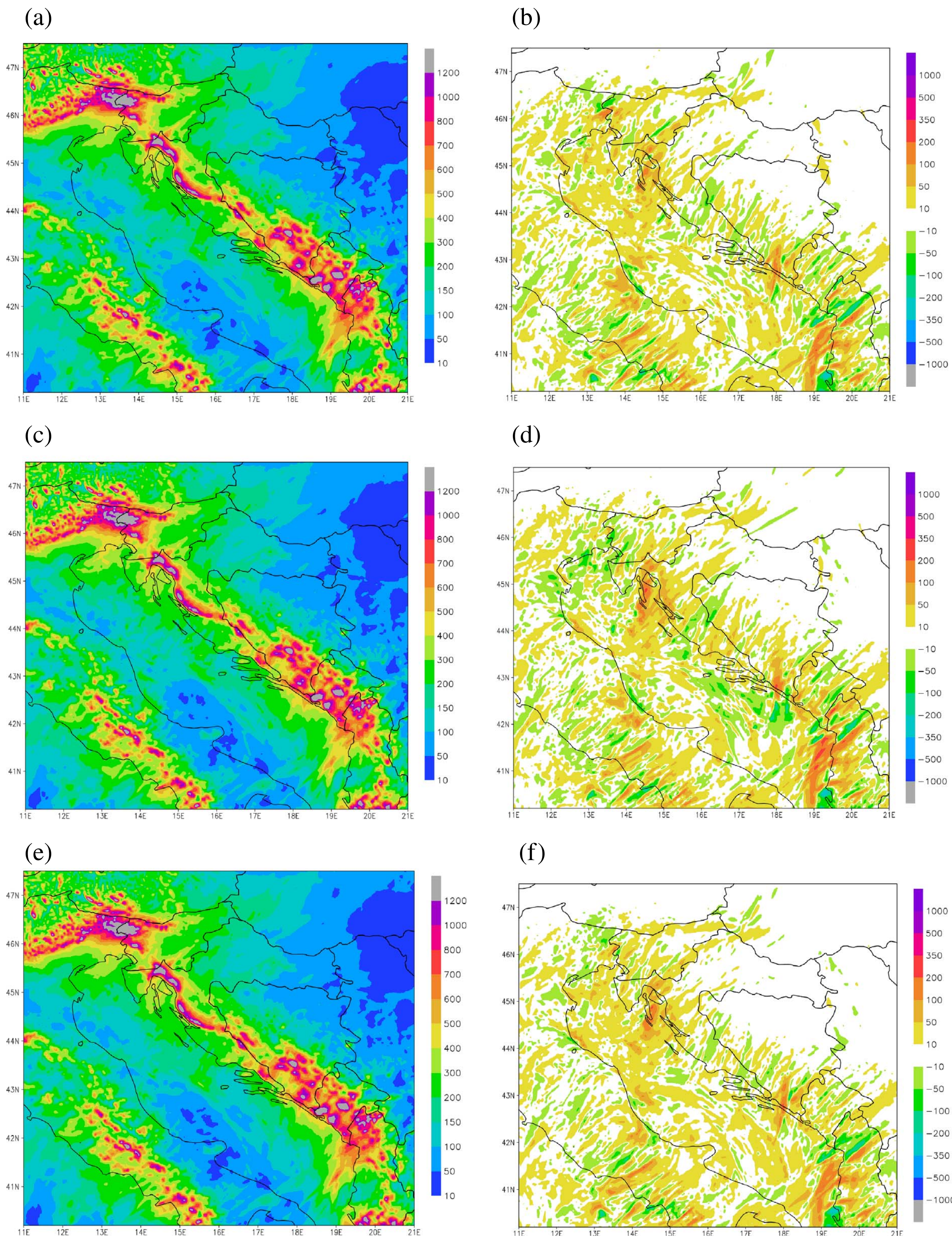

Fig. 10. Precipitation (mm) accumulated during 61 days of SOP1 from 2 km resolution forecasts using SST from: OSTIA (a, b), ROMS (c, d) and MUR (e, f), accumulated values (a, b, c) and difference to the reference (b, d, f).

3.5. Surface fluxes

Fig. 11 shows surface temperature, 2 m temperature, relative humidity and wind speed from model forecasts in 2 km resolution during HyMeX SOP1. The values are averaged over a square with corners at longitude and latitude coordinates SW (14.7,44.7) NE (15.0,45.2) using only values over the sea points.

Fig. 12 shows total fluxes of heat (sensible + latent), turbulent flux of momentum and total water flux (precipitation + evaporation) from model forecasts in 2 km resolution during HyMeX SOP1. The values are averaged over a square with corners at longitude and latitude coordinates SW (14.7,44.7) NE (15.0,45.2) using only values over the sea

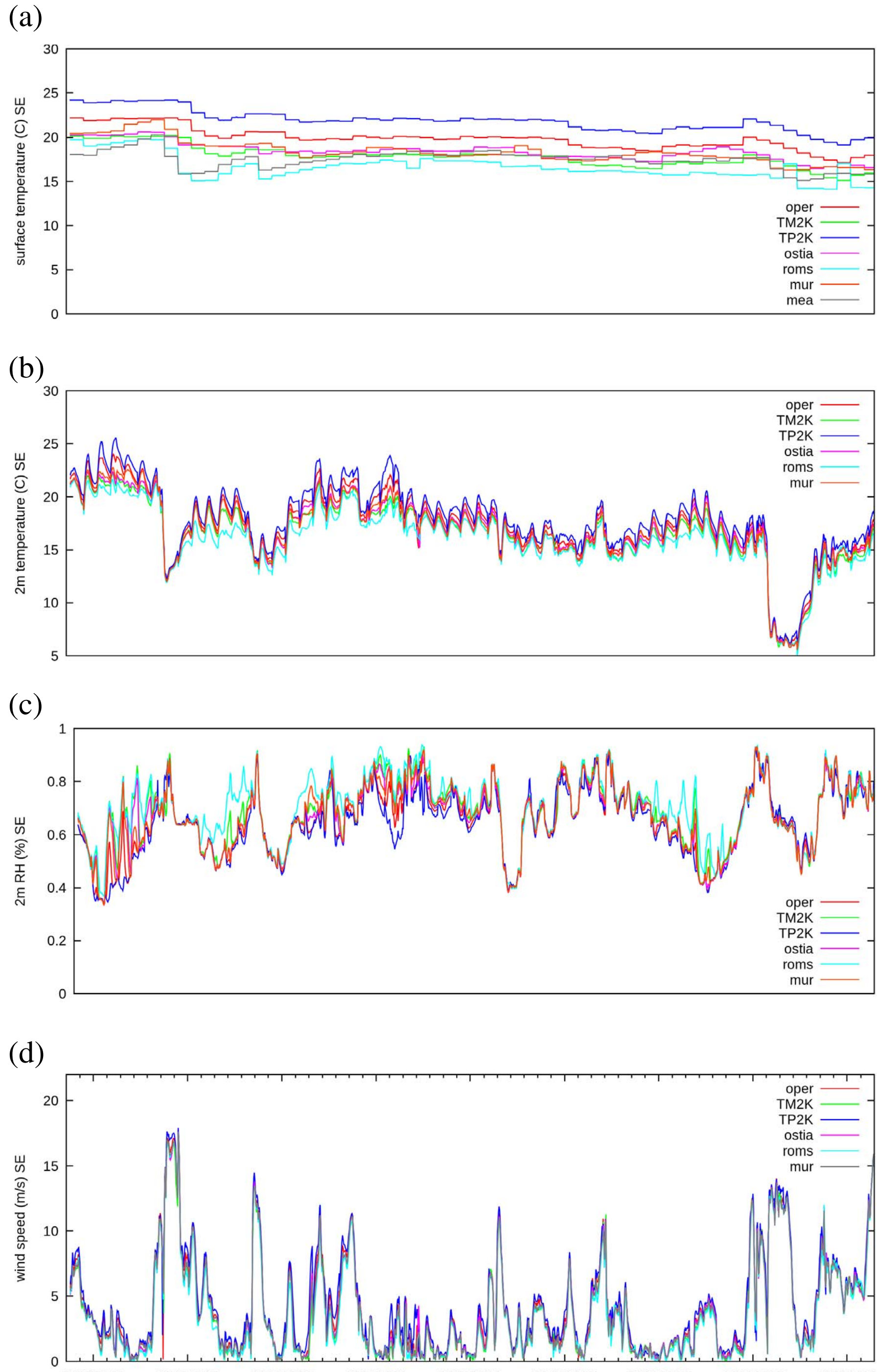

Fig. 11. Surface temperature, 2 m temperature and relative humidity and wind speed from model forecasts in 2 km resolution during HyMeX SOP1. The values are averaged over a square with corners at longitude and latitude coordinates SW (14.7,44.7) NE (15.0,45.2) using only values over the sea points. SE stands for Senj area, mea stands for SST nudged towards measured values.

points.

Surface fluxes are more intensive with higher SST. Heat fluxes from the ocean to the atmosphere (taken negative in Fig. 12) increase twofold from ROMS experiment (with the coldest SST, see Fig. 11) to experiment TP2K. The effect of SST change on other fluxes is less dramatic. Turbulent fluxes of momentum also increase with rising SST (Fig. 12), but the differences are more subtle. Both evaporation (negative water flux in Fig. 12) and precipitation increase with higher SST. Therefore, precipitation is more intensive during IPEs and evaporation is more intensive during bura events.

The differences in surface fluxes between experiments in 8 km resolution are shown in Fig. 13 and in 2 km resolution in Fig. 14. The fluxes of evaporation, sensible and latent heat are negative, so negative difference means that fluxes in OPER are larger. The accumulated 24 hourly fluxes of evaporation, sensible and latent heat reflect the differences in SST. Positive differences in SST yield more evaporation (evaporation flux is negative, Figs. 13 and 14g, h and i), larger sensible and latent heat fluxes. The momentum flux is more complex. Momentum flux is determined by the wind strength as much as by the stability of the lowest layer of the atmosphere. Differences in momentum flux are larger in areas with strong wind (both positive and negative, Fig. 13j, k and l). However, warm SST also enhances vertical mixing and transport of momentum downwards, therefore momentum flux is larger with warmer SST. The OPER experiment has substantially larger momentum fluxes along north-east Adriatic coast than OSTIA, ROMS and MUR experiments, especially in 2 km resolution (Fig. 14j, k

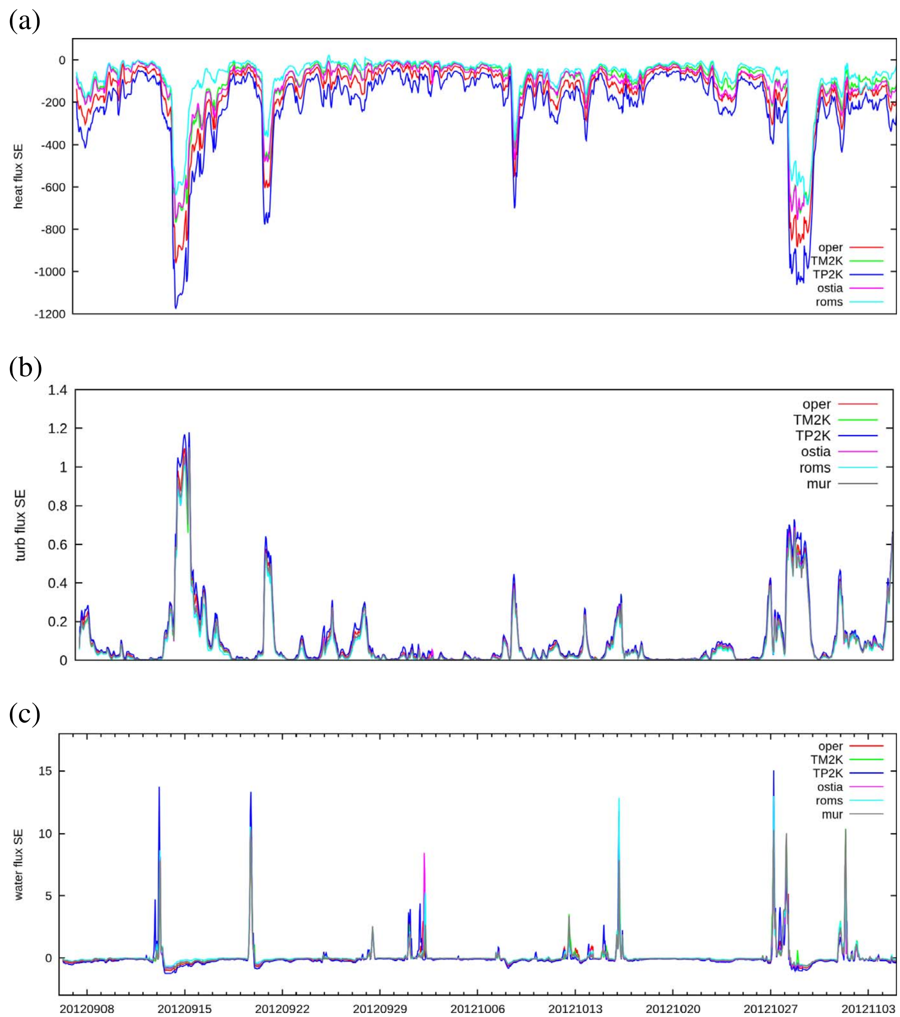

Fig. 12. Total hourly fluxes of heat (sensible + latent W/m^2), turbulent flux of momentum (kg m/s^2) and total water flux (precipitation + evaporation, mm/h) from model forecasts in 2 km resolution during HyMeX SOP1. The values are averaged over a square with corners at longitude and latitude coordinates SW (14.7,44.7) NE (15.0,45.2) using only values over the sea points. SE stands for Senj area.

and l).

3.6. Impact on precipitation for IOP 2

Here we show results for one case of IPE during HyMeX SOP1. Out of 8 cases of IPE that affected eastern Adriatic coast during SOP1, 6 of them affected Rijeka area (Ivančan-Picek et al., 2016), therefore this case is chosen to represent the effect of changing SST to IPE. The reference experiment in the 8 km resolution is the operational forecast. For the whole period of HyMeX SOP1, operational forecast in 8 km resolution does simulate well developed convective systems, which are rich in moisture and generously pouring precipitation over different parts of eastern Adriatic coastline. The reference run simulates the meteorological environment and the development of the convective system for each case, but success of the precipitation forecast varies between cases and consecutive forecast runs.

The location of precipitation maximum in the operational forecast is situated more inland than the observed one. In order to distinguish the contribution of the change in SST from other factors, all experiments start from the operational analysis and only SST values are modified. The same initial conditions are used for the operational run and all experiments, except the SST that was modified using data from different sources. The temperature and moisture on the lowest levels in the atmosphere remain the same as for the initial conditions in the operational forecast and adapt to the new SST conditions during the forecast run. Lower SST moves the precipitation upstream and closer to the coastline while higher SST moves precipitation higher on the mountain slopes. Lower SST stabilizes lower layers of the atmosphere, moist air has less energy to ascend the slope before releasing precipitation.

The operational run starting from the 00 UTC analysis on 11 September 2012 does forecast the position of maximum precipitation correctly (Fig. 15b). Subsequent operational forecasts are less successful in forecasting the position of precipitation maximum and move it northwest. The accumulated 24 hourly precipitation and its differences between experiments are shown for the 2nd day of simulation (precipitation is accumulated from 30 to 54 h forecast that started at 00 UTC of the previous day, Fig. 15). When SST from analyses or ocean model is used (result for ROMS experiment is shown), the spatial distribution of precipitation is very similar to the operational forecast. The main factor determining the precipitation pattern in this case is the atmospheric flow and the mountains. However, the plot showing the difference between the two precipitation fields (Fig. 15d) reveals that the precipitation maximum actually shifts southeastward (upstream). This small shift in the location of precipitation maximum exists already in OSTIA experiment (not shown). This shift contributes to local increase of precipitation in Rijeka and Kvarner Bay. The local precipitation maximum in Rijeka and Kvarner is further enhanced in ROMS experiment (Fig. 15e). Consequently, ROMS experiment enhances precipitation over Kvarner Bay more than OSTIA (ROMS is colder there than OSTIA, while OSTIA is already colder than ARPEGE SST). Using MUR analysis (Fig. 15f) has a similar effect as OSTIA. Nudging OSTIA SST towards insitu measurements has rather small effect (not shown). The precipitation band in MUR experiment is not only shifted upstream, precipitation is more concentrated in a narrow band stretching

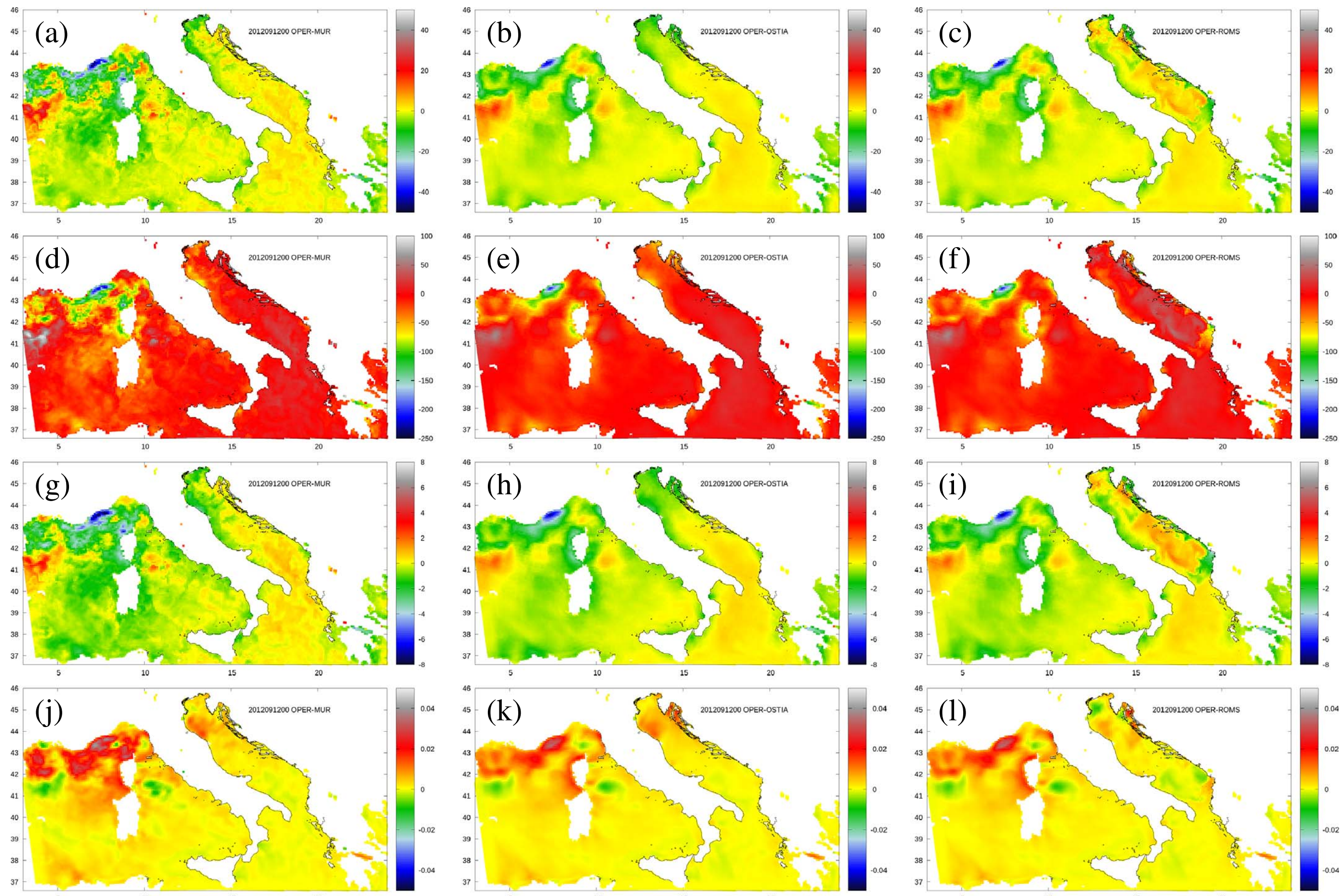

Fig. 13. Differences of the accumulated 24 hourly fluxes for 12 September 2012 from 8 km resolution forecasts: sensible (a, b, c) and latent heat flux (d, e, f) in J/m^2/day, evaporation flux (g, h, i) in mm/day and turbulent momentum flux (j, k, l) in kg m/s/day, experiments OPER-MUR (a, d, g, j), OPER-OSTIA (b, e, h, k) and OPER-ROMS (c, f, i, l).

southeast from Rijeka on its northwest end. Finally, TRMM data (Fig. 15a) show more rain over central Adriatic than predicted by any experiment.

The high resolution reference forecasts precipitation maximum over Rijeka and inland (Fig. 16). This run uses initial and lateral boundary conditions from the operational 8 km resolution run from 00 UTC 12 September 2012. That particular 8 km resolution run forecasts the maximum precipitation over Slovenia and northeastern Italy. One can interpret this improvement in localization as a benefit gained by higher resolution and better representation of topography and islands. In the experiments with alternative SSTs, precipitation pattern is rather similar. The differences in precipitation reveal that part of the precipitation shifts 20–50 km, yielding stripes in the precipitation difference. As expected, the differences are the largest at locations of precipitation maxima, such as at the border between Slovenia and Italy and inland of Rijeka, and exceed 50 mm/24 h (both positive and negative). The river catchments in the area are rather narrow, hence this shift affects which river catchment is expected to receive excess precipitation.

3.7. Categorical verification

In this section, statistical parameters are computed using data measured insitu (TRMM data are omitted). The precipitation data is divided into three categories, thus defining three different events. An event is defined as dry if the 24 h accumulated precipitation on the rain gauge station is less than or equal to 0.2 mm. The threshold between medium and strong rainfall is determined as 95th percentile during the whole SOP1 period at all available stations (the dry events are excluded), which is equal to 50.42 mm accumulated in 24 h. Rain gauge measurements are compared to the modeled 24 h accumulated precipitation at the closest model point (from 06 UTC to 06 UTC on the next day). Up-scaling of 2 km resolution model forecast to 8 km grid is performed in order to reduce the problem of different horizontal resolution models having different sensitivity to double-penalty effect. The marginal distribution of the measurements (climatology) is known as the base rate (BR). It is a characteristic of the forecasting situation (not the forecast system), but rather important for the interpretation of the results. For instance, a lot of verification measures are sensitive to BR, having the higher value for a common event than for a rare one. The extreme example, known as the Finley affair, is percent correct measure of accuracy described by Wilks (2011). In general, the event is easier to forecast if the climatological probability is close to zero or unity than if it is close to 0.5 (Jolliffe and Stephenson, 2012). During the SOP1, the dry event has the highest BR, while strong precipitation is quite rare (happens only in 1.8% occasions, Table 3). Since this measure is independent on the exact forecast, the BR for a single event is the same for different 8 km and 2 km resolution experiments (Tables 3 and 4, the first row).

The frequency bias (FB) compares the frequency of the event forecast with the frequency of the observed event, represented as a ratio. Unbiased forecast exhibits the value of one, indicating the same number of times that the event is predicted as it is observed. Bias greater than one indicates that the event is predicted more often than observed (overforecasting or overestimation), while value less than one indicates that the event is forecast less often than it is observed (underforecasting or underestimation) (Wilks, 2011). The OPER ALADIN 8 km forecast overestimates the frequency of medium precipitation, while the

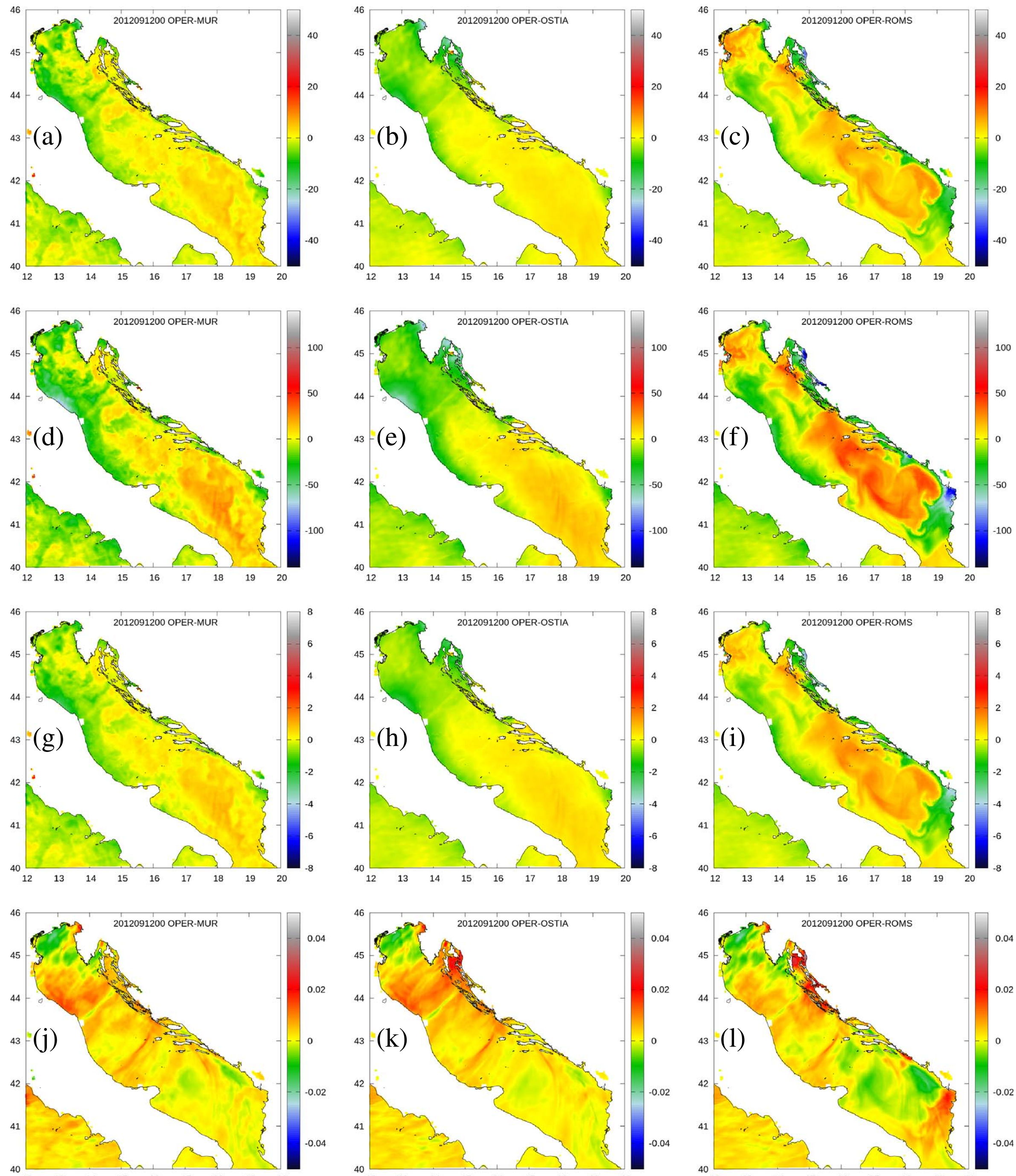

Fig. 14. Differences of the accumulated 24 hourly fluxes for 12 September 2012 from 2 km resolution forecasts: sensible (a, b, c) and latent heat flux (d, e, f) in J/m^2/day, evaporation flux (g, h, i) in mm/day and turbulent momentum flux (j, k, l) in kg m/s/day, experiments OPER-MUR (a, d, g, j), OPER-OSTIA (b, e, h, k) and OPER-ROMS (c, f, i, l).

frequencies are underestimated for the other two events. The overforecast of medium precipitation and underforecast of the dry event is even more evident for OSTIA, MUR and ROMS. On the other hand, OSTIA and MUR overestimate the frequency of strong precipitation, while ROMS predicts this event almost as often as it occurs.

The probability of detection (POD) can be regarded as the fraction of those occasions when the event occurred on which it is also forecast. The POD varies from zero to one (the larger, the better), perfect forecast having the value of one. The false alarm rate (FAR) or the probability of false detection is the ratio of false alarms to the total number of non-occurrence of the event. The FAR has negative orientation, so smaller values are preferred. The best possible value is zero, while the worst possible value equals one.

Jointly, the POD and FAR can be related to the critical success index (CSI). The CSI (also known as threat score) is the number of correctly predicted events divided by the total number of occasions on which that event is forecast and/or observed. It is positively oriented measure of accuracy and it varies from zero (the worst possible forecast) to one (the best possible forecast). It is useful when there is an event that occurs substantially less frequently than other predefined events, even though it is sensitive to base rate (Wilks, 2011). The CSI is the highest for the most common category (dry), and this is the direct consequence of the sensibility of this measure to underlying climatology. The medium precipitation events seem to be the best detected, due to

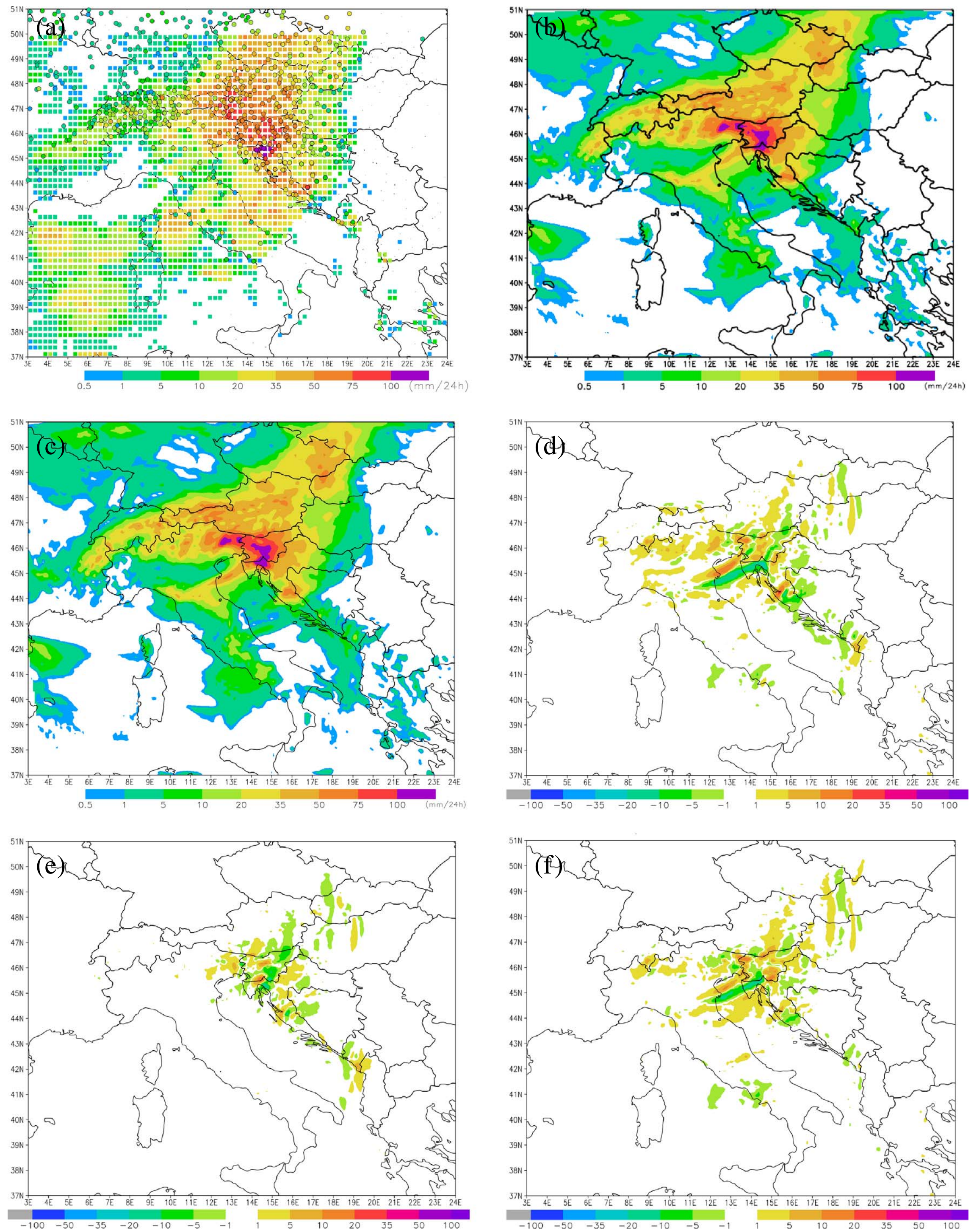

Fig. 15. Accumulated 24 hourly precipitation starting from 06 UTC 12 September 2012, measured (a) from rain gauges (circles) and TRMM estimate (squares), and forecasts: operational (b), ROMS experiment (c) and their difference (d), the difference between OSTIA and ROMS experiments (e) and between OPER and MUR experiments (f) for the 8 km resolution domain, all runs starting from 00 UTC 11 September 2012.

overforecasting of this event. Also, the strong precipitation seems to be the hardest one to predict, with the smallest probability of detection, as well as the highest FAR. But, if the results for different SST are compared, it can be seen that the best results are achieved for OPER. Even though OSTIA, MUR and ROMS predict the strong (and medium) precipitation more often and increase probability of detection (POD), they also increase the FAR. Consequently, the CSI is actually smaller if compared to OPER.

The differences between OPER, OSTIA, MUR and ROMS are much smaller for ALADIN 2 km resolution (Table 4) than for ALADIN 8 km resolution forecasts. This means that ALADIN 2 km is less sensitive to perturbations of SST. The OPER 2 km resolution is less biased than OPER ALADIN 8 km resolution for all events considered. Due to higher FB than for ALADIN 8 km, ALADIN 2 km has higher POD and FAR for dry event, while for medium precipitation FB, FAR and POD are smaller. In general, the CSI value is the same or higher for ALADIN 2 km than for ALADIN 8 km forecasts. This shows that by increasing the resolution of the model and improving physics all the events are more

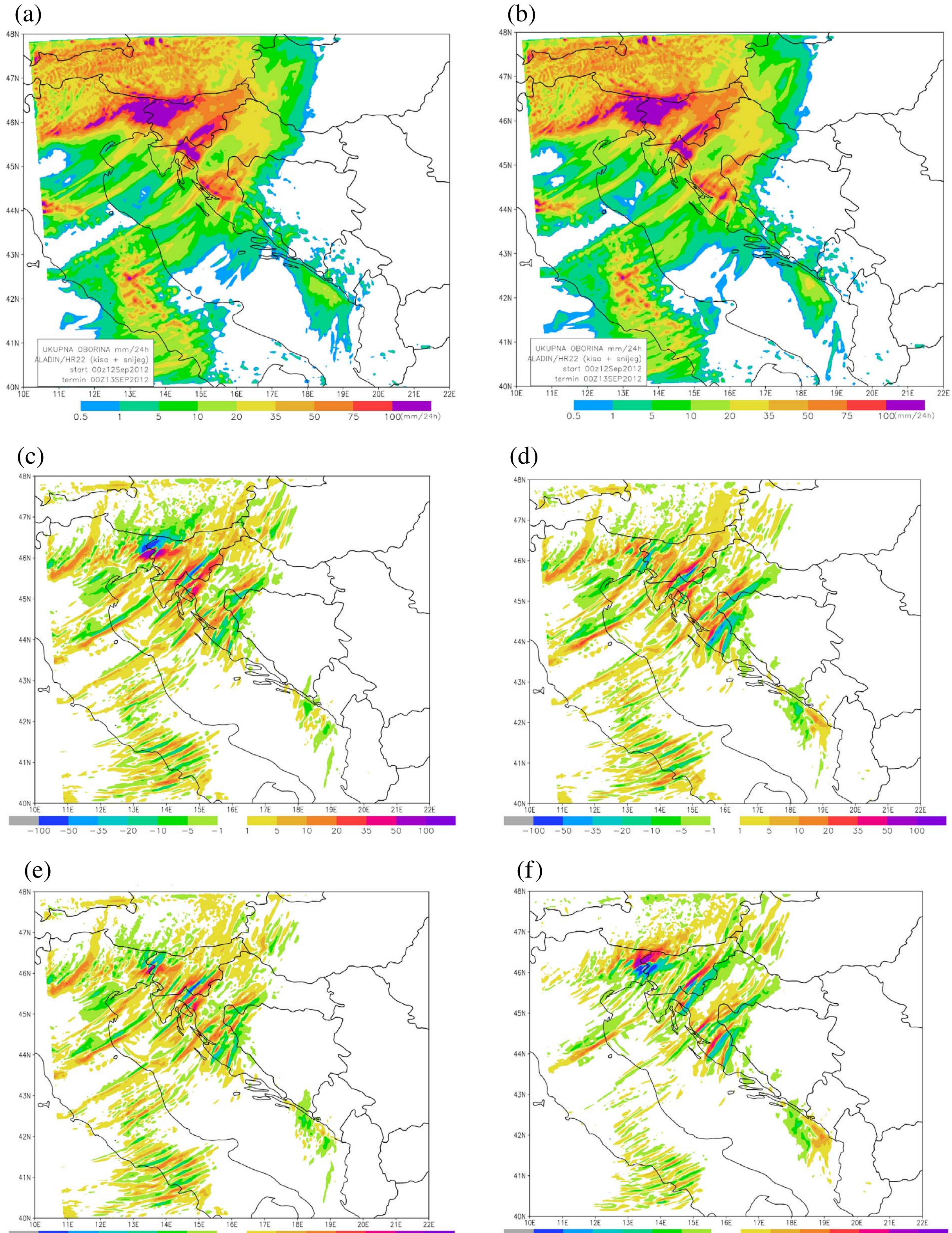

Fig. 16. Accumulated 24 hourly precipitation starting from 06 UTC 12 September 2012 from 2 km resolution forecasts: reference (a), ROMS experiment (b), difference REF-OSTIA (c), REF-ROMS (d), REF-MUR (e) and OSTIA-ROMS (f).

accurately predicted, regardless of their BR.

Up-scaling is performed for ALADIN 2 km, hence the effect of increased sensitivity to the 'double penalty effect' because of the higher resolution is reduced, as previously mentioned. If compared to OPER experiment, by modifying the SST for ALADIN 2 km resolution forecasts, FB changes only for strong precipitation event. For modified ALADIN 2 km resolution forecasts, the strong precipitation FB is the closest to one for ROMS SST, but still overestimating the frequency of strong precipitation more than for ALADIN 8 km forecasts. The smaller the FB in OSTIA, MUR and ROMS SST ALADIN 2 km resolution

Table 3
The ALADIN 8 km resolution experiments base rate (BR), frequency bias (FB), probability of detection (POD) or hit rate (HR), false alarm rate (FAR) and critical success index (CSI) verification measures calculated for different 24 h accumulated precipitation events during the SOP1 period (5 September to 6 November 2012).

Experiment	OPER			OSTIA			MUR			ROMS		
Event	Dry	Medium	Strong	Dry	Medium	Strong	Dry	Medium	Strong	Dry	Medium	Strong
BR (%)	64.9	33.4	1.8	64.9	33.4	1.8	64.9	33.4	1.8	64.9	33.4	1.8
FB	0.78	1.45	0.61	0.73	1.53	1.12	0.73	1.52	1.07	0.73	1.52	1.01
POD/HR	0.76	0.94	0.25	0.71	0.92	0.28	0.71	0.92	0.27	0.71	0.93	0.26
FAR	0.03	0.35	0.59	0.02	0.39	0.75	0.03	0.39	0.74	0.02	0.39	0.74
CSI	0.74	0.62	0.19	0.70	0.58	0.15	0.70	0.58	0.15	0.70	0.58	0.15

forecasts, the smaller the POD, while FAR is almost the same. This means that modification of SST in these cases reduces the frequency of forecast strong precipitation events, but also reduces the correctly forecast ones.

The differences in verification scores between forecasts that use different SST are small. In the experiments, only the initial SST is modified while the rest of the atmosphere adapts to this condition during the forecast. It takes (forecast) time to adapt. The tuning of operational LAM used here was done using the operational SST from ARPEGE (including the convection triggering). Consequently, the spatial distribution of precipitation seems better when assessed subjectively, and new SST field is more realistic, even though the differences in verification measures are small. The differences in the accumulated precipitation over 61 days are small compared to the total amounts. Finally, it needs to be mentioned that the verification measures are highly sensitive to the errors in space and/or time, and that there are considerable areas with no insitu measurements.

4. Summary and conclusions

Adriatic sea is surrounded by mountains that often receives substantial amounts of precipitation in short time (24 h). These heavy precipitation events are a result of air-sea interactions and influence of mountains on atmospheric flow. The SST affects the fluxes between the atmosphere and the sea. The effect on evaporation in a modeling study is found to be lower (Davolio et al., 2017) than the effect on the fluxes of momentum, latent and sensible heat. As a consequence, the vertical profiles are changed and the interaction with the downstream mountains is modified.

First, the SST provided in the global model and analyses is compared to insitu measurements. The first result shows that SST provided by the global models can contain considerable errors (that can reach 10 °C). The global SST analyses also do not reflect local variability in SST, neither in space nor time. In general, there are locations, atmospheric and ocean conditions when ROMS model SST fits insitu measurements of SST better than analyses. Here we show that the SST used in operational NWP model is overestimated for up to 10 °C in Velebit Channel and Rijeka Bay during HyMeX SOP1.

Afterwards we analyze the influence of SST on overall precipitation field that is dominated by IPEs during HyMeX SOP1. The effect of SST on intensity and location of precipitation maxima is explored in 8 and 2 km resolution on IPEs that affect the coastline of the eastern Adriatic. The location of maximum precipitation is more dependent on SST than for the cases analyzed in Davolio et al. (2016).

In the experiments with uniform shift of SST, the overall precipitation does increase/decrease with the increase/decrease of SST. More detailed analysis shows that this is mostly due to the increase of convective precipitation over the sea surface and stratiform on the surrounding mountains. However, the southern Alpine slopes facing the Po valley actually receive less precipitation when SST increases. This is because more convection is triggered over the sea surface (due to warm surface), leaving less moisture to precipitate when reaching the mountain slope. In 2 km resolution, another effect can be seen on the Velebit mountain. When SST decreases, precipitation changes from convective to stratiform, reducing the total precipitation. Colder sea surface evaporates less, triggers less convection and gives less buoyancy to the air parcel above.

The situation is different in the Kvarner bay because there is no valley on the shore of the eastern Adriatic before the mountains. The existence of cold air pool depends on the SST in Kvarner Bay that is much warmer in operational atmospheric model than in reality. This sea surface also contains several islands that pose substantial topographic obstacles for the low level flow. Colder sea surface in the Kvarner Bay and VC contributes to enhanced precipitation over Rijeka area. Consequently, operational high resolution forecast substantially overestimate the precipitation intensity over Velebit mountain. Also, reducing SST enhances precipitation for Rijeka area where maximum precipitation is indeed recorded.

The air parcel attained buoyancy through condensation and released condensates through precipitation. Higher SST yields more precipitation over the sea surface, especially more convective precipitation. Lower SST reduces precipitation by reducing convection, particularly the most intensive one. However, even in the experiment when SST is reduced by 10 °C convective precipitation is not suppressed completely.

Introducing SST from analysis or ROMS model changes the location of the precipitation maximum and enhances precipitation for Rijeka area for IPE analyzed here. But the precipitation forecast over the whole SOP1 period does not change systematically with the introduction of either OSTIA, MUR, ROMS or measured SST (it is neither better nor worse). Most of the IOPs that affect Adriatic during HyMeX SOP1 also affect Rijeka. The operational SST in Kvarner Bay and VC is too warm,

Table 4
The ALADIN 2 km experiments base rate (BR), frequency bias (FB), probability of detection (POD) or hit rate (HR), false alarm rate (FAR) and critical success index (CSI) verification measures calculated for different 24 h accumulated precipitation events during the SOP1 period (5 September to 6 November 2012). The precipitation fields were up-scaled to ALADIN 8 km grid before computing the scores (see text for details).

Experiment	OPER			OSTIA			MUR			ROMS		
Event	Dry	Medium	Strong	Dry	Medium	Strong	Dry	Medium	Strong	Dry	Medium	Strong
BR (%)	64.9	33.4	1.8	64.9	33.4	1.8	64.9	33.4	1.8	64.9	33.4	1.8
FB	0.96	1.07	1.28	0.96	1.07	1.21	0.96	1.07	1.18	0.96	1.07	1.15
POD/HR	0.87	0.79	0.37	0.88	0.79	0.34	0.88	0.80	0.34	0.87	0.80	0.33
FAR	0.09	0.26	0.71	0.09	0.26	0.72	0.09	0.25	0.71	0.09	0.26	0.72
CSI	0.80	0.62	0.19	0.81	0.62	0.18	0.81	0.63	0.18	0.81	0.63	0.18

as shown when compared to the measurements. Analyses have lower SST there, but still higher than the measured values. The ROMS model SST is the closest to the measured values for Rab, Senj and Bakar stations, and the coldest as well. The sea in VC and Kvarner is substantially colder than the surrounding open sea. This supports formation of a cold air pool over Kvarner. Warm and moist air from south/southeast is forced above this cold air pool and this in turn triggers precipitation. Too warm SST over Kvarner Bay and VC in the operational forecast leads to more intensive evaporation from the sea surface. Atmosphere is moister and less stable due to warm surface hence more precipitation is triggered. The two processes act in a similar way. Operational run yields more precipitation over Kvarner due to warmer SST.

Warmer SST (TP5K, TP2K experiments) also means higher air temperature, lower relative humidity and larger amplitude of the diurnal cycle in 2 m temperature. There are fewer clouds in the forecast with warmer SST, particularly the low level cloudiness (cloud fields are not shown, but more clouds are associated with lower amplitude of the diurnal cycle of temperature). Wind speed is affected by the change in SST only marginally, but the forecasts using the lowest SST also show the lowest value of wind speed (and vice versa). The same argument can be drawn for the turbulent momentum fluxes. Fluxes of heat are more intensive with higher SST, especially when wind is strong. Precipitation fluxes over the period of SOP1 are dominated by short intensive events where TP2K (Fig. 12) usually yields most intensive precipitation, but OSTIA and ROMS experiments yield most precipitation in one IPE each.

Statistical analysis did not show substantial improvement in the precipitation scores arising from more realistic SST. The statistical scores are computed using precipitation data measured insitu over land.

As mentioned in the introduction, a simple precipitation increase with SST is sometimes expected (e.g. Pastor et al., 2001). However, the experiments performed with a uniform shift in SST show that the effect on precipitation is not systematic. Although the precipitation over the domain increases with SST, there is less precipitation on the slope of the mountain (the northern slopes of the Po valley). The shift of the maximum precipitation location has been already observed in previous studies. The influence of SST to HPEs is not limited to the contribution of moisture through evaporation of the sea surface. The SST influences the lower portions of the atmosphere, especially the PBL and affects the atmospheric profiles.

Acknowledgments

The Group for High Resolution Sea Surface Temperature (GHRSST) Multi-scale Ultra-high Resolution (MUR) SST data were obtained from the NASA EOSDIS Physical Oceanography Distributed Active Archive Center (PO.DAAC) at the Jet Propulsion Laboratory, Pasadena, CA (https://doi.org/10.5067/GHGMR-_4FJ01). The authors are grateful for the useful comments provided by two anonymous reviewers and Jose Luis Sánchez. This work represents a contribution to the HyMeX international program. The study has been supported in part by the Croatian Science Foundation under the Projects ADAM-ADRIA (IP-2013-11-5928).

References

Acker, J.G., Leptoukh, G., 2007. Online analysis enhances use of NASA earth science data. Eos, Trans. AGU, 88 (2).

ALADIN International Team, 1997. The ALADIN project: mesoscale modelling seen as a basic tool for weather forecasting and atmospheric research. WMO Bull. 46, 317–324.

Bahurel, P., Dombrowsky, E., Lellouche, J.M., Team, Mercator Project, 2004. Mercator ocean monitoring and forecasting system, near-real time assimilation of satellite and insitu data in different operational ocean models. In: Paper Presented at 36Th Colloquim on Ocean Dynamics, Geohydrodyn. and Environ. Res. Group. Univ of Liége, Liége, Belgium.

Bénard, P., Vivoda, J., Mašek, J., Smolíkova, P., Yessad, K., Smith, C., Brožková, R., Geleyn, J.-F., 2010. Dynamical kernel of the ALADIN-NH spectral limited-area model: revised formulation and sensitivity experiments. Quart. J. R. Meteorol. Soc. 136, 155–169. http://dx.doi.org/10.1002/qj.522.

Berthou, S., Mailler, S., Drobinski, P., Arsouze, T., Bastin, S., Béranger, K., Lebeaupin Brossier, C., 2014. Prior history of Mistral and Tramontane winds modulates heavy precipitation events in Southern France. Tellus A 66, 24064. http://dx.doi.org/10.3402/tellusa.v66.24064.

Berthou, S., Mailler, S., Drobinski, P., Arsouze, T., Bastin, S., Béranger, K., Lebeaupin Brossier, C., 2015. Sensitivity of an intense rain event between an atmosphere-only and atmosphere ocean regional coupled model: 19 September 1996. Q. J. R. Meteorol. Soc. 141, 258–271. http://dx.doi.org/10.1002/qj.2355.

Berthou, S., Mailler, S., Drobinski, P., Arsouze, T., Bastin, S., Béranger, K., Flaounas, E., Lebeaupin Brossier, C., Somot, S., Stéfanon, M., 2016. Influence of submonthly air-sea coupling on heavy precipitation events in the Western Mediterranean basin. Q. J. R. Meteorol. Soc. 142, 453–471. http://dx.doi.org/10.1002/qj.2717.

Brožkova, R., Derková, M., Belluš, M., Farda, A., 2006. Atmospheric forcing by ALADIN/MFSTEP and MFSTEP oriented tunings. Ocean Sci. 2, 113–121.

Cassola, F., Ferrari, F., Mazzino, A., Miglietta, M.M., 2016. The role of the sea on the flash floods events over Liguria (Northwestern Italy). Geophys. Res. Lett. 43, 3534–3542. http://dx.doi.org/10.1002/2016GL068265.

Catry, B., Geleyn, J.F., Tudor, M., Bénard, P., Trojakova, A., 2007. Flux conservative thermodynamic equations in a mass-weighted framework. Tellus, Ser. A 59, 71–79.

Charnock, H., 1955. Wind stress on a water surface. Quart. J. Roy. Meteorol. Soc. 81, 639–640.

Chin, T.M., Milliff, R.F., Large, W.G., 1998. Basin-scale, high-wavenumber sea surface wind fields from a multiresolution analysis of scatterometer data. J. Atmos. Oceanic Tech. 15, 741–763.

Davies, H.C., 1976. A lateral boundary formulation for multi-level prediction models. Quart. J. R. Met. Soc. 102, 405–418. http://dx.doi.org/10.1002/qj.49710243210.

Davolio, S., Henin, R., Stocchi, P., Buzzi, A., 2017. Bora wind and heavy persistent precipitation: atmospheric water balance and role of air-sea fluxes over the Adriatic Sea. Q. J. R. Meteorol. Soc. 143, 1165–1177. http://dx.doi.org/10.1002/qj.3002.

Davolio, S., Stocchi, P., Carniel, S., Benetazzo, A., Bohm, E., Ravaioli, M., Riminucci, F., Li, X., 2015. Exceptional Bora outbreak in winter 2012: validation and analysis of high-resolution atmospheric model simulations in the northern Adriatic area. Dynam. Atmos. Oceans 71, 1–20.

Davolio, S., Volonté, A., Manzato, A., Pucillo, A., Cicogna, A., Ferrario, M.E., 2016. Mechanisms producing different precipitation patterns over North-Eastern Italy: insights from hymex-SOP1 and previous events. Q. J. Roy. Meteor. Soc. http://dx.doi.org/10.1002/qj.2731.

Donlon, C.J., Martin, M., Stark, J., Roberts-Jones, J., Fiedler, E., Wimmer, W., 2012. The operational sea surface temperature and sea ice analysis (OSTIA) system. Remote Sens. Environ. 116, 140–158.

Dorman, C.E., Carniel, S., Cavaleri, L., Sclavo, M., Chiggiato, J., Doyle, J., Haack, T., Pullen, J., Grbec, B., Vilibić, I., Janeković, I., Lee, C., Malačić, V., Orlić, M., Paschini, E., Russo, A., Signell, R.P., 2007. February 2003 marine atmospheric conditions and the bora over the Northern Adriatic. J. Geophys. Res. 112, C03S03. http://dx.doi.org/10.1029/2005JC003134.

Doswell, C.A., Brooks, H.E., Maddox, R.A., 1996. Flash flood forecasting: an ingredients-based methodology. Wea. Forecasting 11, 560–581.

Drobinski, P., Ducrocq, V., Alpert, P., Anagnostou, E., Béranger, K., Borga, M., Braud, I., Chanzy, A., Davolio, S., Delrieu, G., Estournel, C., Filali Boubrahmi, N., Font, J., Grubišić, V., Gualdi, S., Homar, V., Ivančan-Picek, B., Kottmeier, C., Kotroni, V., Lagouvardos, K., Lionello, P., Llasat, M.C., Ludwig, W., Lutoff, C., Mariotti, A., Richard, E., Romero, R., Rotunno, R., Roussot, O., Ruin, I., Somot, S., Taupier-Letage, I., Tintore, J., Uijlenhoet, R., Wernli, H., 2014. Hymex: A 10-year multidisciplinary program on the Mediterranean water cycle. Bull. Amer. Meteor. Soc. 95, 1063–1082. http://dx.doi.org/10.1175/BAMS-D-12-00242.1.

Ducrocq, V., Braud, I., Davolio, S., Ferretti, R., Flamant, C., Jansa, A., Kalthoff, N., Richard, E., Taupier-Letage, I., Ayral, P.A., Belamari, S., Berne, A., Borga, M., Boudevillain, B., Bock, O., Boichard, J.L., Bouin, M.N., Bousquet, O., Bouvier, C., Chiggiato, J., Cimini, D., Corsmeier, U., Coppola, L., Cocquerez, P., Defer, E., Drobinski, P., Dufournet, Y., Fourrié, N., Gourley, J.J., Labatut, L., Lambert, D., Le Coz, J., Marzano, F.S., Molinié, G., Montani, A., Nord, G., Nuret, M., Ramage, K., Rison, B., Roussot, O., Said, F., Schwarzenboeck, A., Testor, P., Van Baelen, J., Vincendon, B., Aran, M., Tamayo, J., 2014. Hymex-SOP1, the field campaign dedicated to heavy precipitation and flash flooding in the Northwestern Mediterranean. Bull. Amer. Meteor. Soc. 95, 1083–1100. http://dx.doi.org/10.1175/BAMS-D-12-00244.1.

Dutour Sikirić, M., Janeković, I., Kuzmić, M., 2009. A new approach to bathymetry smoothing in sigma-coordinate ocean models. Ocean Modell. 29, 128–136.

Geleyn, J.F., 1987. Use of a modified Richardson number for parameterising the effect of shallow convection. In: J. Met. Soc. Japan. Special 1986 NWP Symposium Issue, pp. 141–149.

Geleyn, J.F., 1988. Interpolation of wind, temperature and humidity values from model levels to the height of measurement. Tellus, Ser. A 40, 347–351.

Geleyn, J.F., Bazile, E., Bougeault, P., Déqué, M., Ivanovici, V., Joly, A., Labbé, P., Piédeliévre, J.-P., Piriou, J.-M., Royer, J.-F., 1995. Atmospheric parametrization schemes in Météo-France's ARPEGE NWP model. In: Inproceedings of the 1994 ECMWF Seminar on Physical Parametrizations in Numerical Models. ECMWF, Reading, UK, pp. 385–402.

Geleyn, J.F., Bénard, P., Fournier, R., 2005a. A general-purpose extension of the Malkmus band-model average equivalent width to the case of the Voigt line profile. Q. J. Roy. Meteor. Soc. 131, 2757–2768. http://dx.doi.org/10.1256/qj.04.107.

Geleyn, J.F., Fournier, R., Hello, G., Pristov, N., 2005b. A New "Bracketing" Technique for a Flexible and Economical Computation of Thermal Radiative Fluxes, Scattering Effects Included on the Basis the Net Exchanged Rate (NER) Formalism. WGNE Blue Book.

Geleyn, J.F., Váňa, F., Cedilnik, J., Tudor, M., Catry, B., 2006. An Intermediate Solution Between Diagnostic Exchange Coefficients and Prognostic TKE Methods for Vertical Turbulent Transport. WGNE Blue Book.

Geleyn, J.F., Catry, B., Bouteloup, Y., Brožková, R., 2008. A statistical approach for sedimentation inside a micro-physical precipitation scheme. Tellus A 60, 649–662. http://dx.doi.org/10.3402/tellusa.v60i4.15375.

Gerard, L., 2007. An integrated package for subgrid convection, clouds and precipitation compatible with the meso-gamma scales. Quart. J. R. Met. Soc. 133, 711–730. http://dx.doi.org/10.1002/qj.58.

Gerard, L., Geleyn, J.-F., 2005. Evolution of a subgrid deep convection parametrization in a limited-area model with increasing resolution. Quart. J. R. Met. Soc. 131, 2293–2312. http://dx.doi.org/10.1256/qj.04.72.

Gerard, L., Piriou, J.M., Brožková, R., Geleyn, J.-F., Banciu, D., 2009. Cloud and precipitation parameterization in a meso-gamma scale operational weather prediction model. Mon. Wea. Rev. 137, 3960–3977. http://dx.doi.org/10.1175/2009MWR2750.1.

Giard, D., Bazile, E., 2000. Implementation of a new assimilation scheme for soil and surface variables in a global NWP model. Mon. Wea. Rev. 128, 997–1015. http://dx.doi.org/10.1175/1520-0493(2000)128.

Gospodinov, I., Spiridonov, V., Geleyn, J.F., 2001. Second order accuracy of two-time-level semi-Lagrangian schemes. Quart. J. R. Met. Soc. 127, 1017–1033. http://dx.doi.org/10.1002/qj.49712757317.

Grisogono, B., Belušić, D., 2009. A review of recent advances in understanding the meso- and microscale properties of the severe Bora wind. Tellus Vol A 61, 1–16.

Haugen, J., Machenhauer, B., 1993. A spectral limited-area formulation with time-dependent boundary conditions applied to the shallow-water equations. Mon. Wea. Rev. 121, 2618–2630.

Homar, V., Romero, R., Ramis, C., Alonso, S., 2002. Numerical study of the October 2000 torrential precipitation event over eastern Spain: analysis of the synoptic scale stationarity. Ann. Geophys. 20, 2047–2066.

Hortal, M., 2002. The development and testing of a new two-time-level semi-Lagrangian scheme (SETTLS) in the ECMWF forecast model. Q.J.R. Meteorol. Soc. 128, 1671–1687.

Huffman, G.J., Bolvin, D.T., Nelkin, E.J., Wolff, D.B., Adler, R.F., Gu, G., Hong, Y., Bowman, K.P., Stocker, E.F., 2007. The TRMM multisatellite precipitation analysis (TMPA): quasi-global, multiyear, combined-sensor precipitation estimates at fine scales. J. Hydrometeorol. 8, 38–55.

Ivančan-Picek, B., Horvath, K., Strelec Mahović, N., Gajić-Čapka, M., 2014. Forcing mechanisms of a heavy precipitation event in the southeastern Adriatic area. Nat. Hazards 72, 1231–1252. http://dx.doi.org/10.1007/s11069-014-1066-y.

Ivančan-Picek, B., Tudor, M., Horvath, K., Stanešić, A., Ivatek-Šahdan, S., 2016. Overview of the first hymex special observation period over Croatia. Nat. Hazards Earth Syst. Sci. Discuss. http://dx.doi.org/10.5194/nhess-2016-247.

Janeković, I., Mihanović, H., Vilibić, I., Tudor, M., 2014. Extreme cooling and dense water formation estimates in open and coastal regions of the Adriatic Sea during the winter of 2012. J. Geophys. Res. Oceans 119, 3200–3218. http://dx.doi.org/10.1002/2014JC009865.

Jolliffe, I.T., Stephenson, D.B., 2012. Forecast Verification: A Practitioner's Guide in Atmospheric Science, 2nd edition. Wiley and Sons Ltd 274 pp.

MEaSUREs Project, J.P.L.M.U.R., 2015. GHRSST Level 4 MUR Global Foundation Sea Surface Temperature Analysis (V4.1). Ver. 4.1. PO.DAAC, CA, USA. Dataset Accessed [2016-03-01] at http://Dx.Doi.Org/10.5067/{GHGMR}-_4{FJ}04.

Lebeaupin, C., Ducrocq, V., Giordani, H., 2006. Sensitivity of torrential rain events to the sea surface temperature based on high-resolution numerical forecasts. J. Geophys. Res. 111, D12110. http://dx.doi.org/10.1029/2005JD006541.

Manzato, A., Davolio, S., Miglietta, M.M., Pucillo, A., Setvak, M., 2015. 12 September 2012: a supercell outbreak in NE Italy? Atmos. Res. 153, 98–118. http://dx.doi.org/10.1016/j.atmosres.2014.07.019.

Mastrangelo, D., Horvath, K., Riccio, A., Miglietta, M.M., 2011. Mechanisms for convection development in a long-lasting heavy precipitation event over southeastern Italy. Atmos. Res. 100, 586–602. http://dx.doi.org/10.1016/j.atmosres.2010.10.010.

Mazzocco Drvar, D., Plačko-Vršnak, D., Tudor, M., Trošić, T., 2012. Flash-flood in Pula in the night between 24 and 25 September 2010. Cro. Meteorol. Jour. 47, 35–43.

France, Météo, 2012. Joint WMO Technical Progress Report on the Global Data Processing and Forecasting System and Numerical Weather Prediction Research Activities for 2012. 22 pp. availableatwww.wmo.int.

Noilhan, J., Planton, S., 1989. A simple parameterization of land surface processes for meteorological models. Mon. Wea. Rev. 117, 536–549. http://dx.doi.org/10.1175/1520-0493(1989)117.

Oddo, P., Pinardi, N., Zavatarelli, M., Coluccelli, A., 2006. The Adriatic basin forecasting system. Acta Adriat. 47 (Suppl.), 169–184.

Pastor, F., Estrela, M.J., Penarrocha, P., Millan, M.M., 2001. Torreintial rains on the spanish Mediterranean coast: modelling the errect of the sea surface temperature. J. Appl. Meteorol. 40, 1180–1195.

Pullen, J., Doyle, J.D., Hodur, R., Ogston, A., Book, J.W., Perkins, H., Signell, R., 2003. Coupled ocean-atmosphere nested modelling of the Adriatic Sea during winter and spring 2001. J. Geophys. Res. 108 (C10), 3320. http://dx.doi.org/10.1029/2003JC001780.

Pullen, J., Doyle, J.D., Signell, R., 2006. Two-way air-sea coupling: a study of the Adriatc. Mon. Wea. Rev. 134, 1465–1483.

Pullen, J., Doyle, J.D., Haack, T., Dorman, C.D., Signell, R.P., Lee, C.M., 2007. Bora event variability and the role of air-sea feedback. J. Geophys. Res. 112, C03S18. http://dx.doi.org/10.1029/2006JC003726.

Raicich, F., 1994. Notes on the flow rates of the Adriatic rivers. In: Tech. Rep. RF 02/94. CNR Ist. Sper Talassografico, Trieste, Italy.

Rainaud, R., Lebeaupin Brossier, C., Ducrocq, V., Giordani, H., Nuret, M., Fourrié, N., Bouin, M.-N., Taupier-Letage, I., Legain, D., 2016. Characterization of air-sea exchanges over the Western Mediterranean Sea during HyMeX SOP1 using the AROME-WMED model. Q. J. R. Meteorol. Soc. 142, 173–187. http://dx.doi.org/10.1002/qj.2480.

Ricchi, A., Miglietta, M.M., Falco, P.P., Benetazzo, A., Bonaldo, D., Bergamasco, A., Sclavo, M., Carniel, S., 2016. On the use of coupled ocean-atmosphere-wave model during an extreme cold air outbreak over the Adriatic Sea. Atmos. Res. 172-173, 48–65.

Rebora, N., Molini, L., Casella, E., Comellas, A., Fiori, E., Pignone, F., Siccardi, F., Silvestro, F., Tanelli, S., Parodi, A., 2013. Extreme rainfall in the Mediterranean: what can we learn from observations? J. Hydrometeor. 14, 906–922. http://dx.doi.org/10.1175/JHM-D-12-083.1.

Robert, A., 1982. A semi-Lagrangian and semi-implicit numerical integration scheme for the primitive equations. J. Meteor. Soc. Japan. 60, 319–325.

Romero, R., Ramis, C., Alonso, S., 1997. Numerical simulation of an extreme rainfall event in Catalonia: role of orography and evaporation from the sea. Q.J.R. Meteorol. Soc. 123, 537–559.

Senatore, A., Mendicino, G., Knoche, H., Kunstmann, H., 2014. Sensitivity of modeled precipitation to sea surface temperature in regions with complex topography and coastlines: a case study for the Mediterranean. J. Hydrometeorol. 15, 2370–2396.

Shchepetkin, A.F., McWilliams, J.C., 2005. The regional ocean modelling system: a split-explicit, free-surface, topography-following-coordinate oceanic model. Ocean Model 9, 347–404.

Shchepetkin, A.F., McWilliams, J.C., 2009. Correction and commentary on Ocean forecasting in terrain-following coordinates: formuation and skill assessment of the regional ocean modelling system by Haidvogel et al., J. Comput. Phys., 227, 3565-3624. J. Comput. Phys. 228, 8985–9000.

Silvestro, F., Gabellani, S., Giannoni, F., Parodi, A., Rebora, N., Rudari, R., Siccardi, F., 2012. A hydrological analysis of the 4 November 2011 event in Genoa. Nat. Hazards Earth Syst. Sci. 12, 2743–2752. http://dx.doi.org/10.5194/nhess-12-2743-2012.

Simmons, A.J., Burridge, D.M., 1981. An energy and Angular-Momentum conserving vertical finite-difference scheme and hybrid vertical coordinates. Mon. Wea. Rev. 109, 758–766.

Small, R.J., deSzoeke, S.P., Xie, S.P., O'Neill, L., Seo, H., Song, Q., Cornillon, P., Spall, M., Minobe, S., 2008. Air-sea interactio over ocean fronts and eddies. Dyn. Atmos. Ocean. 45, 274–319.

Stanešić, A., 2011. Assimilation system at DHMZ: development and first verification results. Cro. Met. Jour. 44/45, 3–17.

Stark, J.D., Donlon, C.J., Martin, M.J., McCulloch, M.E., 2007. OSTIA : An Operational, High Resolution, Real Time, Global Sea Surface Temperature Analysis System. IEEE, Aberdeen, Scotland.

Stocchi, P., Davolio, S., 2016. Intense air-sea exchange and heavy rainfall: impact of the Northern Adriatic SST. Adv. Sci. Res. 13, 7–12.

Strazzo, S.E., Elsner, J.B., LaRow, T.E., Murakami, H., Wehner, M., Zhao, M., 2016. The influence of model resolution on the simulated sensitivity of North Atlantic tropical cyclone maximum intensity to sea surface temperature. J. Adv. Model. Earth Syst. 8, 1037–1054. http://dx.doi.org/10.1002/2016MS000635.

Termonia, P., 2008. Scale-selective digital filter initialization. Mon. Wea. Rev. 136, 5246–5255.

Toy, M.D., Johnson, R.H., 2014. The influence of an SST front on a heavy rainfall event over coastal Taiwan during tiMREX. J. Atmos. Sci. 71, 3223–3249.

Trenberth, K.E., Shea, D.J., 2005. Relationships between precipitation and surface temperature. Geophys. Res. Lett. 32, 1–4.

Tudor, M., 2013. A test of numerical instability and stiffness in the parametrizations of the ARPÉGE and ALADIN models. Geoscientific model development 6, 901–913.

Tudor, M., 2015. Methods for automatized detection of rapid changes in lateral boundary condition fields for NWP limited area models. Geosci. Model Dev. 8, 2627–2643.

Tudor, M., Ivatek-Šahdan, S., 2010. The case study of bura of 1 and 3 February 2007. Meteorol. Z. 19 (5), 453–466.

Tudor, M., Termonia, P., 2010. Alternative formulations for incorporating lateral boundary data into limited-area models. Mon. Wea. Rev. 138, 2867–2882.

Tudor, M., Ivatek-Šahdan, S., Stanešić, A., Horvath, K., Bajić, A., 2013. Forecasting weather in Croatia using ALADIN numerical weather prediction model. In: Zhang, Y., Ray, P. (Eds.), Climate Change and Regional/Local Responses. InTech, Rijeka, pp. 59–88.

UK Met Office, 2005. GHRSST Level 4 OSTIA Global Foundation Sea Surface Temperature Analysis. Ver. 1.0. PO.DAAC, CA, USA. . Dataset accessed [2016-04-28] at https://doi.org/10.5067/GHOST-_4FK01.

Váňa, F., Bénard, P., Geleyn, J.F., Simon, A., Seity, Y., 2008. Semi-lagrangian advection scheme with controlled damping - an alternative way to nonlinear horizontal diffusion in a numerical weather prediction model. Quart. J. R. Met. Soc. 134, 523–537. http://dx.doi.org/10.1002/qj.220.

Weill, A., Eymard, L., Caniaux, G., Hauser, D., Planton, S., Dupuis, H., Brut, A., Guerin, C., Nacass, P., Butet, A., Cloché, S., Pedreros, R., Durand, P., Bourras, D., Giordani, H., Lachaud, G., Bouhours, G., 2003. Toward better determination of turbulent air-sea fluxes from several experiments. J. Clim. 16, 600–618.

Wilks, D.S., 2011. Statistical Methods in the Atmospheric Sciences, 3rd edition. Elsevier.